Development of a New Biomechanical *ex vivo* Perfusion System

Studies on effects of biomechanical and inflammatory stress on hemostatic genes in human vascular endothelium

Niklas Bergh

Institute of Medicine
at Sahlgrenska Academy
University of Gothenburg

The Sahlgrenska Academy

UNIVERSITY OF GOTHENBURG

From the Clinical Experimental Research Laboratory,
Department of Emergency and Cardiovascular Medicine,
Sahlgrenska University Hospital/Östra,
Institute of Medicine,
The Sahlgrenska Academy at University of Gothenburg,
Gothenburg, Sweden

Development of a New Biomechanical *ex vivo* Perfusion System

Studies on Effects of Biomechanical and Inflammatory Stress on Hemostatic Genes in Human Vascular Endothelium

Niklas Bergh

2009

Development of a New Biomechanical *ex vivo* Perfusion System -
Studies on effects of biomechanical and inflammatory stress on hemostatic genes in human vascular endothelium
ISBN 978-91-628-7891-7

niklas.bergh@gu.se

From the Clinical Experimental Research Laboratory,
Department of Emergency and Cardiovascular Medicine,
Sahlgrenska University Hospital/ Östra,
Institute of Medicine, the Sahlgrenska Academy, University of Gothenburg,
Gothenburg, Sweden

Printed by Geson Hyltetryck, Gothenburg, Sweden, 2009

In memory of my father

ABSTRACT

The vascular endothelium is a multifunctional interface constantly exposed to biomechanical forces such as shear and tensile stress. Biomechanical stress is involved in the pathophysiological process of the vessel wall and thus affects vascular remodeling, atherosclerosis and thrombogenesis. Many different systems have been designed to subject endothelial cells to mechanical stress. However, previous systems have had large limitations in creating physiologically relevant biomechanical stress protocols. Therefore, there is a need for more refined biological perfusion systems that as accurately as possible mimics the *in vivo* conditions. In the present work, a new biomechanical *ex vivo* perfusion system for integrative physiological and molecular biology studies of intact vessels of different sizes as well as artificial vessels was developed.

This model was constructed for advanced perfusion protocols under strictly controlled biomechanical (shear stress, tensile stress) as well as metabolic (temperature, pH, oxygen tension) conditions. The system enables monitoring and regulation of vessel lumen diameter, shear stress, mean pressure, variable pulsatile pressure and flow profiles, and diastolic reversed flow. The vessel lumen measuring technique is based on detection of the amount of flourescein over a vessel segment. A combination of flow resistances, on/off switches and capacitances creates a wide range of possible combinations of pulsatile pressures and flow profiles. The perfusion platform was extensively evaluated technically as well as biologically by perfusion of high precision made glass capillaries, human umbilical arteries as well as endothelialized artificial vessels.

Artificial vessels with a confluent human umbilical vein endothelial cell layer were exposed to different levels of shear stress or different levels of static or pulsatile pressure. Shear stress was a more powerful stimulus than static or pulsatile tensile stress. While shear stress affected mRNA expression of all six studied genes (t-PA, PAI-1, u-PA, thrombomodulin, eNOS and VCAM-1), neither gene was found to be regulated by tensile stress. Shear stress suppressed t-PA and VCAM-1 in a dose response dependent way. The expression of thrombomodulin was also reduced by shear stress. u-PA, eNOS and PAI-1 were induced by shear stress, but showed no obvious dose response effect for these genes. Further, the unexpected suppression of t-PA by shear stress was studied by using mechanistic experiments with pharmacologic inhibitors. Our data indicate that the suppressive effect of shear stress on t-PA was mediated by suppression of JNK and not by p38 MAPK and ERK1/2.

The interplay between inflammatory stress and different combination of tensile as well as shear stress was studied on six key anti- and pro-thrombotic genes in HUVEC. The endothelial cell response to TNF-α was not modulated by tensile stress. Again, shear stress was a more potent stimulus. Shear stress counteracted the cytokine-induced expression of VCAM-1, and the cytokine-suppressed expression of thrombomodulin and eNOS. Shear stress and TNF-α additively induced PAI-1, whereas shear stress blocked the cytokine effect on t-PA and u-PA.

In conclusion, these findings illustrate that biomechanical forces, particularly shear stress, have important regulatory effects on endothelial gene function. A possible pathophysiological scenario is that an unfavourable hemodynamic milieu leads to a lower threshold for the induction of genes related to endothelial dysfunction in lesion-prone areas upon negative stress, such as inflammation.

Key words: *ex vivo* perfusion system, biomechanical, endothelium, shear stress, tensile stress, pulsatile, TNF-α, JNK, hemostatic genes

LIST OF ORIGINAL PAPERS

This thesis is based on the following papers, identified in the text by their Roman numerals:

I Bergh N*, Ekman M*, Ulfhammer E, Andersson M, Karlsson L, Jern S. A new biomechanical perfusion system for *ex vivo* study of small biological intact vessels. * both authors contributed equally
Annals of Biomedical Engineering 2005;33(12):1808-1818.

II Bergh N, Ulfhammer E, Karlsson L, Jern S. Effects of two complex hemodynamic stimulation profiles on hemostatic genes in a vessel-like environment.
Endothelium 2008;15(5-6):231-238.

III Ulfhammer E, Carlström M, Bergh N, Larsson P, Karlsson L, Jern S. Suppression of endothelial t-PA expression by prolonged high laminar shear stress.
Biochemical Biophysical Research Communication 2009;379(2):532-6.

IV Bergh N, Ulfhammer E, Glise K, Jern S, Karlsson L. Influence of TNF-α and biomechanical stress on endothelial anti- and prothrombotic genes.
Biochemical Biophysical Research Communication 2009;385(3):314-318.

CONTENTS

ABBREVIATIONS

AP-1	activator protein-1
ATF-2	activation transcription factor-2
cAMP	cyclic adenosine monophosphate
cDNA	complementary DNA
CRE	cAMP response element
CREB	CRE-binding protein
C_T	threshold cycle
EC	endothelial cell
ELISA	enzyme-linked immunosorbent assay
EMSA	electrophoretic mobility shift assay
eNOS	endothelial nitric oxide synthase
ERK1/2	extracellular receptor-activated kinase – 1 and 2
EtOH	ethanol
GAPDH	glyceraldehyde 3-phospate dehydrogenase
GFP filter	green fluorescent protein filter
HAEC	human aortic endothelial cell
HSS	high shear stress
HUVEC	human umbilical vein endothelial cell
ICAM-1	intercellular adhesion molecule-1
IL-1β	interleukin-1β
JNK	c-jun N-terminal kinase
LSS	low shear stress
MAPK	mitogen activated protein kinase
mRNA	messenger RNA
MSS	moderate shear stress
NF-κB	nuclear factor-κB
NO	nitric oxide
PAI-1	plasminogen activator inhibitor-1
PID	Proportional, Integral, Derivative
PTFE	Polytetrafluoroethylene
RNA	ribonucleic acid
RT-PCR	reverse transcription polymerase chain reaction
SDS	sodium dodecyl sulfate
SSRE	shear stress responsive element
TM	thrombomodulin
TNF-α	tumor necrosis factor-α
TNFR1 & 2	TNF-α receptor 1 & 2
t-PA	tissue-type plasminogen activator
u-PA	urokinase-type plasminogen activator
uPAR	u-PA receptor
VCAM-1	vascular cell adhesion molecule-1

INTRODUCTION

Cardiovascular disease is the leading cause of morbidity and mortality in the western world and during the past decades it has also become an increasing problem in developing countries [1]. Acute events, such as myocardial infarction and ischemic stroke, are usually triggered by the rupture of an atherosclerotic plaque which activates the intravascular clotting cascade causing an event that, when unopposed, rapidly will lead to the formation of a lumen-occluding thrombus. Numerous risk factors for atherosclerosis have been identified, including smoking, hypercholesterolemia, hypertension, autoimmune chronic low grade of inflammatory stress *etc*.

Hemodynamic stress has been suggested to be involved in the pathophysiological processes of the vessel wall, such as vascular remodeling, atherosclerosis and thrombogenesis. Chronically altered mechanical forces, such as hypertension, induces adaptive alterations of vessel wall shape and composition as well as increases the risk of thrombogenesis. Atherosclerotic lesions typically show a distinct, highly diversified pattern of anatomic localization with a predilection to areas with turbulence, flow reversal and low shear stress. Chronic low grade inflammatory stimuli associated with *e.g*. hypertension and rheumatoid arthritis induce endothelial dysfunction which promotes the atherosclerotic process as well as thrombogenesis. Against this background, this thesis focuses on the development of a suitable *ex vivo* perfusion system for studies of biomechanical stress on intact human vessels or isolated endothelial cells, with a special focus on the influence of biomechanical and inflammatory stress on important hemostatic genes.

The vascular wall

The wall of veins and arteries consists of three layers: tunica intima, tunica media and tunica adventitia. The innermost layer is the tunica intima, which consists of a monolayer of endothelial cells lining the lumen of the vessel. The endothelial cell layer is supported by a subendothelial layer of loose connective tissue. Tunica media, the middle layer is composed of smooth muscle cells and extracellular matrix proteins. This layer is much thicker in arteries than in veins. The outer layer, tunica adventitia, is composed of fibroblasts and loose connective tissue.

The vascular endothelium may be regarded as an independent organ dispersed over the entire body [2]. The overall surface of the endothelium has been reported to vary between 350 and 1000 m^2 and with a weight between 0.1 and 1.5 kg [2-4]. The endothelium has an important role as the link between the nutritive blood flow and the metabolically demanding tissue. The endothelium senses mechanical, chemical and humoral stimuli, and responds by synthesis and release of a wide range of biologically active substances. Vascular tone is regulated by release of vasoactive substances such as nitric oxide (NO), prostacyclin (PGI_2), and endothelin-1 (ET-1). Further, the endothelium has a central role in maintenance of blood fluidity by expressing antithrombotic and fibrinolytic properties. Surface-expressed compounds like tissue-fac-

tor pathway inhibitor (TFPI), thrombomodulin (TM), heparin sulphate, ecto-ADPase, and protein S have antithrombotic and anticoagulating properties [5]. The fibrinolytic function includes the release of tissue-plasminogen activator (t-PA) [6, 7] as well as urokinase-type plasminogen activator (u-PA) [8] upon stimulation. The endothelium has a central role in regulating tissue inflammation in response to pro-inflammatory cytokines (TNF-α, IL-1) by altering cell shape and motility in a way that may contribute to increased vascular leakage and leukocyte adhesion through expression of vascular cell adhesion molecule-1 (VCAM-1), intercellular adhesion molecule-1 (ICAM-1) and E-selectin [9].

Biomechanical forces

Mechanical forces related to pressure and flow are crucial in determining blood vessel wall adaptation in normal and diseased states, in arteries as well as in veins [10, 11]. Vascular remodeling may have important clinical implications during the progression of several cardiovascular disorders. These structural changes within the vasculature appear to be associated with changes in endothelial function. Mechanical stress affects vascular remodeling which alter compliance in hypertension, causes vascular fragility and compensatory changes in atherosclerosis [12], leads to restenosis after angioplasty [13] and modulates the thromboprotective state of the endothelium [14, 15]. Understanding how mechanical stress influences the modeling-remodeling processes is particularly critical for developing successful therapies in vascular pathology.

The forces imposed on the vessel wall originate from the intraluminal pressure and the friction of the flowing blood. The hemodynamic forces acting on the vessel wall can be described by two major components, *i.e.* tensile stress and shear stress [16, 17] (Figure 1). Tensile stress is created by the pulsatile blood pressure and results in an

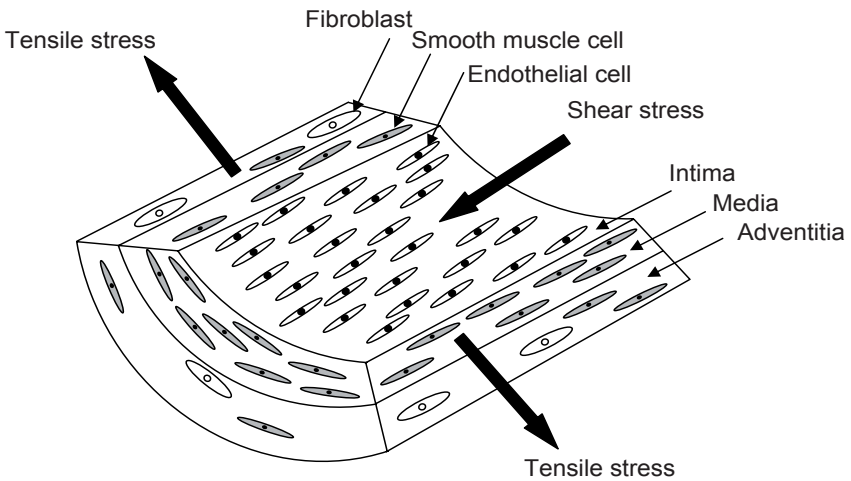

Figure 1. Shear stress and tensile stress are the two major biomechanical forces acting on the vessel wall. Shear stress is the frictional force exerted by the blood flow. Tensile stress is generated by the blood pressure. The vessel wall consists of three layers with endothelial cells, smooth muscle cells and fibroblasts.

elongation of the cell. This force is distributed perpendicular to the blood stream and affects all constituents of the vessel wall. It is proportional to the transmural pressure and inner radius of the vessel and inversely proportional to the vessel wall thickness. Tensile stress in large arteries ranges from 2 to 18% during the normal cardiac cycle [18].

Shear stress is the frictional force imposed on the endothelial cell surface by the flowing blood. It is mainly considered to affect the endothelium which responds to the local flow environment by modulating vascular tone, hemostasis, inflammatory reactions, lipid metabolism, cell growth, cell migration and interactions with extracellular matrix. Shear stress is proportional to the blood flow and viscosity of the blood and inversely proportional to the third power of the radius. Shear stress ranges between 1-6 dyn/cm^2 in veins and 2-40 dyn/cm^2 (locally up to 100 dyn/cm^2) in arteries [2, 16, 19, 20]. Typically, shear stress in the arterial network is actively regulated at a constant level of approximately 15 dyn/cm^2 [16, 17, 21]. Ultimately, this determines blood vessel geometry and function.

The pathways mediating the response of endothelial cells to hemodynamic stimuli are largely unknown. Studies have suggested the importance of shear sensitive ion channels, G-proteins, mechanical traction on endothelial cytoskeleton, integrins, cell-cell-junction (PECAM-1) and adherens junctions (VE-cadherin) [19-21]. Activation of mechanoreceptors releases second messengers such as focal adhesion kinase, phospholipase C and mitogen-activated protein kinase (MAPK) cascades [20]. This in turn leads to activation and translocation of transcription factors to the nucleus. Direct force transmission through the cytoskeleton to different compartments in the cell is another signaling mechanism involved [20, 21].

Methodological challenges in studies of biomechanical forces

It is a great methodological challenge to create suitable experimental models for studies of biomechanical forces. A vast amount of different experimental protocols have been used for mechanical stress studies *in vivo*, *in vitro* and *ex vivo*, each hampered with difficulties to control and monitor the various components of the complex biomechanical stress profile.

In vivo experiments are typically based on perfusion studies of isolated organs, for instance the human forearm [22, 23]. Although *in vivo* models have proved useful in establishing a relation between vascular remodeling and mechanical stress to which blood vessels are subjected, they do not permit clarification of signaling pathways at the cellular level. Nor do they allow distinction between neurohormonal and mechanical effects. An advantage is that pressure and flow conditions are physiologically relevant, however at the same time, this makes it impossible to define the exact force each vessel segment is exposed to. This is particularly true for shear stress, since shearing forces are extremely difficult to measure *in vivo*.

Due to these difficulties, *in vitro* cell culture models have been extensively used and have permitted identification of biomechanical stress components that might affect

smooth muscle and endothelial cell function. For studies on shear stress, the parallel-plate flow chamber [24, 25] and cone-and-plate device systems [26, 27] are some of the most widely used experimental systems. Tensile stress is usually studied by using a device in which the cells are exposed to circumferential stretch [28]. The advantages of *in vitro* systems are that the biomechanical stress can be exactly defined and that the use of molecular biology techniques are more easily applied to cultured cells due to the abundant amount of material that can be obtained. On the other hand, this approach has certain limitations. The *in vitro* culture conditions differ markedly from the *in vivo* micro-environment and endothelial-smooth muscle cell interactions and cell-matrix interactions that could be critical in modulating the cell response are not reproduced. Also, the complex biomechanical stress interactions seen *in vivo* have not been possible to study with traditional flow chambers in which only one stress component may be studied. To overcome some of the limitations of these traditional approaches, *ex vivo* vascular perfusion systems have been developed.

The *in vivo* biomechanical flow situation shows a high grade of complexity which has to be addressed in *ex vivo* systems. However, the technical problems with *ex vivo* perfusion systems have been to regulate and monitor the different types of biomechanical stress. Instead of physiological pulse pressure generation many previous systems have used a sinusoidal pulse wave form and shear stress calculations have only been based on approximations [29, 30]. *In vivo* observations have shown that the endothelium in particular is extremely sensitive to the local biomechanical flow situation. Physiological laminar shear stress is thought to maintain normal endothelial structure and function, whereas turbulent flow, stasis, and local shear gradients may activate endothelial cells and induce a pro-atherogenic state [31, 32]. In particular, a rapidly changing and oscillatory flow with reversing flow directions as well as low net flow rates tend to induce a more pathologic state compared with laminar flow or oscillatory flow that remains unidirectional [30, 31, 33]. Compliance of the underlying vascular wall importantly modulates the consequences of oscillatory flow. Thus, if the vascular wall has normal distensibility, oscillatory flow seems to be cytoprotective, but the same stimulus has an adverse effect in a non-compliant vessel [34, 35]. Increases in pulsation frequency and/or pulse pressure seem to influence endothelial cells in an unfavorable way [36-38]. Increased pressure and flow have profound effects on arterial structure, including increased arterial size through remodeling and effects on growth of new vessels through angiogenesis [39]. Diastolic wave reflection mostly seen in young, healthy adults may eliminate the exposure to repetitive and potentially deleterious diastolic stasis [40]. Furthermore, repetitive short-term increases of pulse pressure, pulse rate, and shear stress appear to contribute to the antiatherosclerotic effects of physical exercise in coronary [41, 42] as well as peripheral arteries [43].

In order to investigate the impact of complex biomechanical stress on the vessel wall, *ex vivo* perfusion systems that meet diverse demands when it comes to combining flow and pressure profiles are required. A great advantage of *ex vivo* systems is that they make it possible to elucidate the impact of different types of biomechanical stress on endothelial gene regulation as well as studies of intra-cellular signaling cascades. Consequently, *ex vivo* perfusion systems with the capacity to control complex biomechanical stress profiles may possibly enhance our knowledge in these issues and increase our understanding of perservation of endothelial function.

Inflammation

Chronic low grade inflammation has proved to be a risk factor for increased morbidity and mortality in cardiovascular disease. Essential hypertension, angina pectoris, intermittent claudication *etc.* may be associated with a low grade of chronic inflammation. Inflammatory stress shifts the hemostatic balance to favor the activation of coagulation. Inflammatory mediators can elevate platelet count, platelet reactivity, down regulate natural anticoagulatory mechanisms, initiate the coagulation system, facilitate propagation of the coagulant response and impair fibrinolysis. In extreme situations, this may lead to either disseminated intravascular coagulation or thrombosis [44]. Chronic low grade inflammatory stress seen in patients with chronic inflammatory diseases, *e.g.* systemic lupus erythematosus and rheumatoid arthritis, is associated with an increased risk for developing myocardial infarction and stroke [45, 46]. Even increased chronic levels of C-reactive protein (CRP) without any other clinical inflammatory symptoms are predictive of cardiovascular events [47]. Since inhibition of tumor necrosis factor-alpha (TNF-α) reduces the incidence of cardiovascular event [48], one suggestion is that the increased incidence is due to some part, being mediated by proinflammatory cytokines. TNF-α is one of the most important promoters of inflammation. It is principally derived from mononuclear phagocytes and endothelial cells are a major cellular target of its action. Exposure of endothelial cells to TNF-α results in activation of three major proinflammatory signaling pathways: the NF-κB pathway, the p38 MAPK pathway and the JNK pathway [9, 49]. These signaling cascades interact through a complex network, which mediates gene regulatory effects primarily by activation of the two transcription factors NF-κB and AP-1 [49, 50].

In unstressed cells NF-κB resides in the cytoplasm because of its association with inhibitor proteins (IκBs). Binding of TNF-α to its receptors (TNFR 1 & 2) results in phosphorylation of IκB by the IκB kinase (IKK) complex [9]. This phosphorylation results in a rapid degradation of IκB and unmasks a nuclear localization sequence of NF-κB making it free to translocate to the nucleus and regulate transcription. In endothelial cells, TNF-α induced NF-κB consists of homo- or heterodimers involving p50, p65, and c-Rel subunit, [9]. AP-1 is a heterogeneous collection of dimeric transcription factors comprising Jun, Fos, and ATF subunits, and is in response to TNF-α an outcome of preferentially JNK and p38 MAPK signaling [50, 51].

Biomechanical stress has been reported to modulate the response in endothelial cells to proinflammatory cytokines (TNF-α, interleukin (IL)-1β). However, the literature is quite sparse and most previous studies have focused on shear stress and leukocyte adhesion genes (VCAM-1, ICAM-1) [52-56]. There are no previous reports that have investigated the synergistic effect between cytokines and tensile stress. The literature is somewhat conflicting regarding the regulatory effect of biomechanical and inflammatory stress on t-PA and PAI-1 [57-59].

Influence of biomechanical and inflammatory stress on vessel wall function

The endothelium has an important role as the active barrier between the nutritive blood flow and the metabolically demanding tissue. It responds by synthesis and re-

lease of a wide range of biologically active substances upon mechanical, chemical and humoral stimulation. Hemodynamic and inflammatory stress influence the development of atherosclerotic lesions, remodel vessel wall, impair endogenous fibrinolysis and increase coagulation. In this thesis, the regulatory capacities of different types of biomechanical stress and/or inflammatory stress were studied in endothelial cells. We selected six key genes within our area of interest to represent the spectrum of some different hemostatic functions of the endothelial cell.

t-PA

The endogenous fibrinolytic system protects the circulation from intravascular fibrin formation and thrombosis. t-PA, a serine protease, is the physiologically most important trigger of fibrinolysis in the vascular compartment. t-PA is synthesized and released by endothelial cells [60-63]. The fibrinolytic process acts as a counter-regulatory mechanism to the coagulation cascade and its main inhibitor is PAI-1 [64, 65]. Other circulating inhibitors of plasminogen activators, such as C1-inhibitor, α2-macroglobulin and α1-antitrypsin are probably of less importance [66, 67]. The crucial regulatory step of the endogenous fibrinolysis is the release of t-PA from endothelial cells, since t-PA is released as an active enzyme. The proteolytic activity of t-PA is greatly enhanced by fibrin, and t-PA associated with fibrin is protected from complex formation with inhibitors. t-PA released and present during thrombus formation is far more potent in inducing clot dissolution than when added after clot formation [60, 62].

The importance of t-PA has been confirmed in animal studies with t-PA deficient mice [68], as well as observed *in vivo* in subjects with impaired capacity for t-PA release due to a polymorphism in the t-PA gene; these individuals were found to have a more than 3-fold increased risk for myocardial infarction [69]. Endothelial cells are the main source of circulating t-PA and the release to plasma follows both a constitutive and a regulated pathway [70]. Upon stimulation by several substances formed during the process of thrombus formation, such as thrombin, bradykinin, factor X and platelet activating factor (PAF), large amounts of t-PA are released from intracellular storage pools [6, 7]. In plasma, only approximately 20% of the t-PA circulates in its free and active form [71-73]. t-PA has a short half-life in plasma, only 3-5 min [74].

u-PA

u-PA has similar catalytic properties as t-PA. In contrast to t-PA, which is the key enzyme in the intravascular fibrinolysis, u-PA has its main function in the extravascular compartment. u-PA is also a serine protease and activates plasmin, through catalyzing the conversion of plasminogen into plasmin, which in turn degrades fibrin [75]. u-PA is active in tissue remodeling and cell migration in wound healing, tumor metastasis, inflammation and atherosclerosis [76-78]. u-PA is secreted from cells and forms a complex with cell membranes through binding the specific cellular receptor urokinase-type plasminogen activator receptor (u-PAR). When binding the receptor, u-PA is cleaved by plasmin and kallikrein to the active form of u-PA [75]. The proteolytic activity of u-PAR bound u-PA is blocked by binding PAI-1 [75]. The u-PA-u-PAR-PAI-1 complex is then internalized into the cells and u-PA is degraded, while u-PAR

is recycled to the cell surface [79, 80]. u-PA is synthesized by many different cell types, *e.g.* smooth muscle cells, macrophages and endothelial cells [8, 81, 82]. u-PA expression is modulated by biomechanical stress, growth factors and cytokines [83]. u-PA has been shown to be overexpressed in atherosclerotic human aortas, carotid arteries and coronary arteries [78, 81]. There is evidence that increased amount of u-PA causes acute vascular constriction, accelerated atherosclerotic lesion growth, and that it seems to break down elastin which could make the arterial wall more prone to aneurysm formation [84, 85].

PAI-1

PAI-1 is the main inhibitor of t-PA and u-PA. It is a serine protease inhibitor (serpin). The interaction between t-PA/u-PA and PAI-1 is very rapid, with a second order rate constant of approximately 10^7 M^{-1} s^{-1} [64]. PAI-1 is synthesized and secreted as an active inhibitor, but is spontaneously converted into a latent, non-inhibitory form [86]. The fraction of active PAI-1 in plasma has been reported to vary between 20 and 90 percent [87-89]. The active form in plasma is stabilized by binding to vitronectin. PAI-1 is present in a several-fold molar excess over t-PA in plasma [90]. The origin of plasma PAI-1 is under debate. PAI-1 is produced by a variety of cells in culture and is widely distributed in many tissues *in vivo*. *In vitro* PAI-1 can be synthesized by endothelial cells, smooth muscle cells, macrophages, hepatocytes, adipocytes and even platelets [91-93]. Our group has shown that plasma PAI-1 in healthy lean individuals probably originates from platelets [94, 95]. Furthermore, Schleef *et al.* reported that the majority of PAI-1 associated with cultured human endothelial cells was located beneath the cells in the extracellular matrix [96] indicating that PAI-1 synthesized in endothelial cells might be more important in regulating subendothelial fibrinolysis. In contrast to t-PA, PAI-1 is not stored in endothelial cells. PAI-1 has been shown to be regulated by a number of different factors including lipoproteins, glucose, cytokines, thrombin, growth factors and insulin [97]. *In vivo* elevated plasma level of PAI-1 is a common feature of the insulin resistance syndrome, and show correlations with obesity, hyperlipidemia, hyperinsulinemia, hypertension *etc*. [98, 99]. In this condition there are indications that the fat tissue is the main source of plasma PAI-1 levels [95].

TM

Thrombomodulin (TM) is an integral membrane protein expressed on the surface of endothelial cells. The main function of TM is to act as a cofactor in the thrombin-induced activation of the anticoagulant protein C pathway. TM binds thrombin with high affinity and results in >1000-fold amplification of the rate of protein C activation [100]. The procoagulant properties of thrombin are lost on binding to TM since TM occupies the functionally important exosite I in thrombin and thereby blocks interactions with other thrombin binding proteins. The protein C system together with its cofactor protein S provides an important control of blood coagulation through inhibiting coagulation by degrading FVIIIa and FVa on the surface of negatively charged phospolipid membranes [100, 101]. Furthermore, the TM-thrombin complex has an antiinflammatory, antiapoptotic function and promotes fibrinolysis by cleaving the thrombin activatable fibrinolysis inhibitor (TAFI) into its active form. The rate limit-

ing step is the interaction of thrombin with TM [101]. The entire vascular endothelium expresses TM, the concentration being particularly high in the capillaries where the ratio between the endothelial cell surface and blood volume reaches its peak [100]. TM is also expressed by astrocytes, keratinocytes, mesothelial cells, neutrophils and platelets [101].

eNOS

eNOS plays an important role in maintaining vascular tone and integrity. It is considered to be a vasoprotective molecule [102]. Mice with homozygous eNOS deletion are prone to develop hypertension and ischemia-induced tissue damage [103, 104]. eNOS is expressed in endothelial cells in the entire vasculature. The protective action of eNOS is attributed to its catalysis of nitric oxide (NO), a radical that diffuses extracellular and targets subendothelial smooth muscle cells and blood platelets. NO is produced from arginine and oxygen in a variety of mammalian cell types by three distinct NOS (nitric oxide synthase) isozymes: the two constitutively transcribed forms neuronal NOS (nNOS) and endothelial NOS (eNOS) enzymes, and an inducible form (iNOS) found in a number of cell types including macrophages and vascular smooth muscle cells [104]. NO is a highly reactive molecule and excessive NO production causes cell damage. Therefore the catalytic action of eNOS is tightly regulated [102]. Augmented NO production at vascular sites possesses inhibitory actions against inflammation, vascular remodeling, smooth muscle proliferation and myocardial damage. The catalytic activity of eNOS is stimulated by various physical and chemical stimuli such as shear stress, thrombin, histamine and bradykinin, [102] and suppressed by hypertension, dyslipidemia and smoking [105].

VCAM-1

VCAM-1 is an endothelial adhesion molecule of the Ig gene superfamily that participates in atherogenesis by promoting monocyte, lymphocyte, eosinophil and basophil granulocyte accumulation in the arterial intima [106]. VCAM-1 has important roles in the development of atherosclerosis and rheumatoid arthritis. VCAM-1 is not constitutively expressed under physiological conditions. However, under pro-inflammatory conditions, expression of VCAM-1 is rapidly increased by the vascular endothelium [105]. VCAM-1 may also be expressed on macrophages, myoblasts and dendritic cells. VCAM-1 interacts with integrin $\alpha 4\beta 1$ on rolling and tethering leucocytes. The integrin-VCAM-1 interaction triggers changes in shape of the endothelial cells allowing leukocytes to migrate extravascular [105, 107]. Mice with homozygous VCAM-1 deficient domains have significantly reduced early atherosclerotic lesions although cholesterol levels, lipoprotein profiles and numbers of circulating leukocytes were comparable to wild-types [106]. *In vivo*, VCAM-1 is unique in that its expression is largely restricted to atherosclerotic lesions and lesion-predisposed regions, whereas the other major adhesion molecule, ICAM-1, is expressed in lesions-predisposed as well as in uninvolved regions [106].

AIMS

Against this background the objective of the present work was to:

- develop a new vascular experimental perfusion platform for integrative physiological and molecular biological studies of small intact biological or artificial endothelialized vessels (Paper I)

- create a system which enables prolonged perfusion of biological vessels under strictly controlled biomechanical (shear stress, tensile stress) as well as metabolic (temperature, pH, oxygen tension) conditions (Paper I)

- biologically and technically validate the capacity of the system (Paper I and II)

- study the effects of complex hemodynamic stimulation profiles on hemostatic gene expression in a vessel-like environment (Paper II)

- further investigate the underlying mechanism beyond the shear stress suppressive effect on t-PA found in paper II (Paper III)

- investigate the interaction between biomechanical stress and simultaneous proinflammatory stress by the cytokine TNF-α on the expression of anti- and prothrombotic genes in endothelial cells (Paper IV)

STUDY OVERVIEW

Paper I

The first study is a methodological evaluation of the new *ex vivo* perfusion system developed by us. This new experimental platform enables perfusion of small intact vessels or artificial vessels with a confluent endothelial cell layer. The biomechanical flow profile and the metabolic environment are strictly controlled and regulated by in house developed software.

Paper II

The second study is a further development and biological evaluation of the perfusion system. In this study confluent endothelial cells seeded in silicone tubes or glass capillaries were exposed to different levels of tensile stress (static/pulsatile) or different levels of shear stress. The gene regulatory effect of different biomechanical stress profiles was studied on six central hemostatic genes.

Paper III

The third study focuses on the unexpected finding in Paper II that shear stress suppresses t-PA in a dose-dependent way. To verify these results a similar shear stress study was performed in a commercially available perfusion system, the Streamer^{TM} device (Flexcell). Further, this study aimed at elucidating by which intracellular mechanism this suppressive effect is mediated.

Paper IV

The fourth study was designed to investigate the interplay between biomechanical stress and inflammatory stress on central hemostatic genes. Confluent endothelial cells were exposed to the combination of different biomechanical stress profiles (similar as in Paper II) and the proinflammatory cytokine TNF-α, which was added to the perfusion medium.

THE PROCESS OF DEVELOPMENT OF A NEW BIOMECHANICAL *EX VIVO* PERFUSION SYSTEM

The new biomechanical *ex vivo* perfusion model

The fundamental task was to develop a novel *ex vivo* perfusion system in which the advantages from previous *in vitro*, *in vivo* and *ex vivo* systems could be combined. The aim was to develop a platform that enabled us to combine, generate, regulate and monitor virtually any biomechanical stress profile.

The perfusion system was designed to meet the following specifications:

- perfusion of intact vessels with a diameter range of 1-4 mm and a length of 10-15 cm
- two parallel perfusion circuits independently regulated and monitored
- static pressure regulation
- a pulsatile profile regulation in terms of pulse pressure, frequency, duration, and systolic and diastolic waveform morphology
- diastolic reversed flow regulation
- continuous measurement of diameter at different positions of the vessel
- shear stress monitoring and regulation at different positions of the vessel
- regulation of pH, pO_2, and temperature

Overview of the *ex vivo* perfusion model that was developed

The perfusion system consists of two separate perfusion circuits. Each perfusion circuit enables perfusion of up to three different vessels separately controlled. An overview of one of the perfusion circuits is shown in Figure 2. Each perfusion circuit has a

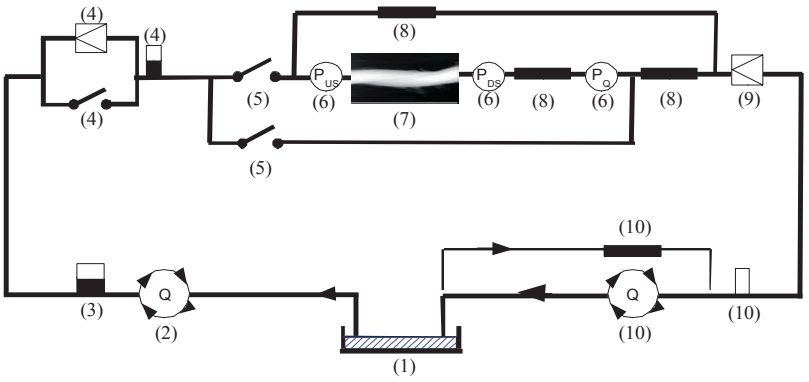

Figure 2. The system consists of two parallel perfusion circuits which are separately controlled. One of the two circuits is shown in the overview. (1) reservoir; (2) inlet pump; (3) pre-pressurized reservoir; (4) on/off switch, variable resistance and capacitance for pulse profile shaping; (5) on/off switches for flow direction control; (6) pressure transducers, (7) perfusion chamber monitored by a video system, (8) flow resistances, (9) variable flow resistance; (10) resistance, sub pressure reservoir, sub-pressure pump and outlet.

perfusate reservoir placed in a temperature-controlled water bath (Grant GD100/S12, VWR international AB, Stockholm, Sweden). The perfusate is driven by a high precision tubing pump (Ismatec IPC, Labinett AB, Gothenburg, Sweden), controlled by the software. Downstream of the inlet pump is a static pre-pressurized reservoir. An operator-defined pulsatile profile is generated by a variable flow resistance (Bürkert 2821, Fluid Control Systems, Malmö, Sweden), a circuit on/off switch (Bürkert 2821), and a variable capacitance. A diastolic flow reflection wave is generated by leading the perfusate the opposite way through the vessel by controlling the opening and closing of two different circuits on/off switches. Intraluminal pressure is measured by pressure transducers (DPT-600, Triplus, Gothenburg, Sweden) up- and downstream of the vessel. Volume flow through the vessel is calculated by measuring the pressure drop over a resistance in serial with the vessel. Intraluminal mean pressure level is regulated by a variable flow resistance (Bürkert 2821) downstream the vessel. To be able to maintain any desired mean vessel pressure there is a sub pressure unit downstream of the variable flow resistance, consisting of an outlet and sub pressure pump (Ismatec IPC), a sub pressure reservoir, and a parallel flow resistance.

Each perfusion circuit has a superfusate reservoir placed in a temperate water bath (the same as for the perfusate reservoirs). The superfusate is circulated by a tubing pump (Ismatec IPC). Before reaching the vessels, both the perfusate and superfusate pass through a final specially designed heat exchanger (Department of Medical Technology SU/Östra, Gothenburg, Sweden) to ensure constant temperature of 37° ± 0.1°C. pH and pO_2 is continuously monitored and regulated by administration of CO_2 and O_2 in the perfusate and superfusate reservoir.

The custom-designed vessel perfusion chamber (Department of Medical Technology) hosts two vessels, two reference capillaries and 100 ml superfusate for each vessel. The vessel perfusion chamber, final heat exchanger, pressure transducers, pulse dampers, resistances, and temperature sensors are enclosed in a dark temperature controlled chamber (Department of Medical Technology). The perfusion chamber is placed under a microscope (Olympus SZX 12, Olympus Optical AB, Solna, Sweden), equipped with a video camera (Sony ExwaveHAD) and a mercury lamp (Olympus U-LH100Hg Olympus Optical AB, Solna, Sweden), for excitation and recording of emitted fluorescing light. This is used for diameter measurement.

Vessel

The aim was to create a system allowing perfusion of a wide range of different vessels. However, it was necessary to restrict the vessel lumen to less than 4 mm in the actual setups because of the capacities of the tubing pumps, Luer connections and electromagnetic valves. To be able to perfuse larger vessels in the future, the dimension of the different parts of the circuits need to be modified.

The initial focus was to use intact human vessels. Human umbilical arteries were used as a prototype in the evaluation of the system. However, these vessels turned out to be inconvenient for further biological studies since most arteries were in an extremely contracted mode which was hard to reverse. A wide range of different smooth muscle

cell relaxing substances as well as endothelial dependent vasodilator substances were evaluated with a success rate of one vessel out of six.

Other suitable vessels were searched for with no success. Optimal vessels would have been human vessels with no major curvatures or branches, minimizing the risk for turbulence or a non-laminar flow profile. The left internal mammary artery, LIMA, may be an optimal vessel for future studies.

Since we had no success in finding an appropriate intact human vessel, we decided to start working with artificial vessels. Two different vessel chambers were used for silicone tubes and glass capillaries, respectively. The dimension of the silicone tubes and glass capillaries were chosen to have a comparable intra luminal surface area.

Component sustainability

All the different components in the perfusion circuits were carefully tested and controlled to be non-toxic for biological tissue. All surfaces exposed to the perfusion circuit should remain intact during the autoclave process (*i.e*. high temperature and pressure) and resist 70% EtOH perfusion. Preferentially, all parts should be flow-dynamically optimized, to minimize the risk for appearance of locus that are vulnerable for contamination or deposition of salt crystals. It was hard to find magnetic valves insensitive for deposition of salt crystals and pH electrodes resistant to EtOH as well as the autoclave process.

Metabolic conditions

To assure well controlled and regulated metabolic conditions, in despite of the surrounding temperature, flow conditions *etc*., we initially sought to incorporate the whole system into a CO_2 incubator. However, this turned out to be unsuccessful since the electronic equipment could not withstand the humidified air and the pumps, valves *etc.* generated too much heat disabling the temperature control of the incubator. Instead, we constructed a temperature controlled chamber. Since all components did not fit into the chamber we had to assure that in despite of flow velocity, the temperatures of the super- as well as the perfusate were at the required temperature when it reached the vessels. This required careful testing of the construction of the final heat exchanger and placement of the temperature measurement electrodes. The super- and the perfusate circuits were optimized to need as little perfusion volume as possible.

pH and pO_2 is measured by pH and pO_2 electrodes connected to WTW pH 340i meters (Christian Berner AB, Gothenburg, Sweden) and regulated in the system by intermittent bubbling of CO_2 and O_2, respectively. The regulation of gas delivery through syringe filters with 0.2-µm PTFE membranes (Life Sciences, Sweden) to each circuit is separately controlled by the computer through gas valves (Bürkert 2821). The bubbling of gas into the perfusion medium caused problems since this resulted in intensive foaming of the serum containing medium (Paper II-IV). We did not want to reduce the serum levels since this could affect the endothelial cells. Different outlet syringe filters were tested but they all clotted immediately by the bubbles. We solved

this by optimizing the gas delivery to be as small as possible and replacing the syringe filters with an EtOH-lock where the gas bubbles could pass through. There was a natural delay between gas delivery and response in pH/pO_2 which the regulation algorithm had to compensate for. Extensive evaluating work were performed in optimizing the regulation routines of the gas valves (valve extrapolation factor, valve opening duration, valve delay, valve sensitivity, derivate evaluation smooth factor) which finally assured a stable pH/pO_2. Before as well as after perfusion the super- and perfusates were analyzed for endotoxin and microbiological contamination.

Pressure regulation

The pressure regulation has to be calibrated prior to each experiment. The intraluminal pressure immediately before (P_{US}) and after (P_{DS}) the perfusion chamber is recorded by pressure transducers (DPT-600) which are calibrated simultaneously with a pneumatic pressure transducer calibrator, through an automatic calibration routine in the software, which keeps the maximum inter-transducer variability below 0.001 mmHg. The mean intraluminal pressure is calculated (P_{US} + P_{DS})/2 and regulated by a variable flow resistance (Bürkert 2821). During the development we had large problems in finding a suitable flow resistance since the most common variable flow resistances on the market were constructed with an electromagnetic piston. The problem with the piston constructed valves was that these were extremely sensitive to deposition of salt crystals, proteins *etc*., resulting in malfunctioning of the valve. Finally, we found a variable flow resistance in which no critical moving parts came into contact with the perfusate but instead worked through an elastic silicone membrane which was extended into the lumen. The software regulation parameters for the variable flow resistance were crucial in achieving a stable and fast enough regulation function as well as preventing internal pressure oscillations. The calibration parameters were optimized to different flow rates and saved in different calibration files for predefined flow intervals.

We constructed the flow circuits to minimize the flow resistance. This was important in order to enable high volume flows and concomitant intraluminal pressure close to zero. It was a matter of priority how large tubings that could be accepted, since the larger tubing we chose, the lower the flow resistance would be, while the turn-over time of the medium in the tubes increased, especially during low flow stimulations. We optimized the ratio between the flow resistance contra medium turn-over in the tubes and we also created a so-called sub pressure unit downstream of the perfusion chamber. This unit lowers the overall resistance in the circuits.

In the final version a variable flow resistance in parallel with an on/off switch followed by a capacitance is used to induce pulsations. The timing of the switch (pulsatile rate, systolic/diastolic duration, position and duration of pulse wave reflection) is controlled by the operator through the software. The capacitance is used to control the diastolic phase. The volume of the capacitance can be used to create different diastolic profiles. To learn how we could control the pressure profile we had to create numerous different combinations of flow resistances, different regulation loops for the on/off switch and capacitances.

Flow direction

The flow direction through the vessel is regulated by two on/off switches. The timing of the switches is independently controlled, with an accuracy of 10 ms. Different forward and reversed flow, turbulence and pressure profiles can be generated by different combinations of flow resistances and timing of the switches.

Measurement of vessel diameter

The precision of the shear stress calculation is critically dependent on the precision of the measurement of the vessel lumen diameter. In the shear stress formula the lumen diameter is raised to the third power and small errors in lumen measurements results in large shear stress deviations. One limitation of many previous perfusion systems is that the shear stress calculation, if implemented at all, has been based on the average diameter of the whole vessel [108, 109]. We thought that this was an essential drawback since numerous reports have reported that shear stress has important gene regulatory effects. We aimed at creating a system admitting continuous measurements of the diameter at different loci of the vessel, *e.g*. up- and downstream of a stenosis.

Creating a method that enabled measuring the internal lumen diameter precisely turned out to be one of the most difficult tasks of the developing work. Also, the method should enable diameter measurements within different segments of the vessel. One of our first approaches was to use ultrasonographic measurements. This turned out to be an unreliable method since it was impossible to synchronize the ultrasonographic apparatus software with the software controlling the perfusion system. Further, our aim was to be able to measure at different loci simultaneously which would require multiple probes which the apparatus could not handle. Our next step was to try to visualize the intraluminal space through an edge-detection system. We placed the perfusion chamber under a microscope with a wide-angle objective and connected a video camera to the microscope which digitized the image and fed it into the software for image analysis. The lumen of the vessels were visualized by fluorescein isothiocyanate dextran, 150 kDa molecular weight (FITC-dextran, Sigma, St Louis, MO; USA). The FITC-dextran was stable for more than 24 h and it had a Stokes radius of approximately 85 Å which was large enough to prevent any leakage through the vessel wall, even in the presence of endothelial damage. However, this was also an unreliable method since we had problems in establishing a calibration method for the edge-detection and there was poor correlation between the luminal diameter controlled by ultrasonographic measurement. The inexactness of the method was in large part due to the uncontrolled dispersion of the light from excited FITC-dextran in the vessel wall as well as light scattering during passage between different medium (liquid/gas).

To bypass this problem, we had to construct a method independent of luminal wall detection and therefore we created an indirect method to measure the inner diameter. In the final version, the diameter of a defined segment of the vessel is calculated from the corresponding intraluminal volume of the segment. FITC-dextran is added to the perfusion medium and the intraluminal volume is determined by quantifying the amount of emitted light within the selected segment of the vessel. The amount of emitted light from this segment is proportional to the volume of the segment (Figure 3).

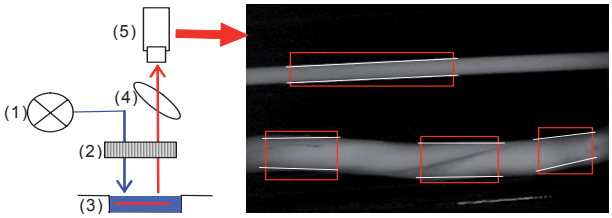

Figure 3. A schematic of vessel lumen imaging and measurement of the vessel diameter. A mercury lamp excites the FITC-dextran in the vessel lumen. The emitted light passes through a GFP-light filter and is recorded by the video camera and transferred to the computer. The operator has chosen to place three different ROIs over the vessel. Within each ROI, light is quantified from which mean lumen diameter within the ROI is determined. At the top of the picture is the reference capillary with a ROI placed over it. (1) mercury lamp; (2) GFP-light filter; (3) perfusion chamber; (4) microscope; (5) video camera attached to the microscope.

Fluorescein is excited through the vessel wall by the mercury lamp attached to the microscope. The peak of excitability is at 480 nm and the emission peak is at 525 nm. The emitted light passes through a light-filter (GFP-filter, Chroma Technology Corporation, Brattleboro, USA) to eliminate any interfering background light. The emitted light is detected by the computer through the video camera attached to the microscope. The light is quantified by the software within a region-of-interest (ROI) of the segment of the vessel as defined by the operator. The length of the vessel segment within the ROI is measured by the software. The frequency of diameter measurement up-dating is set by the operator, so the vessel is only exposed to the ultraviolet emission for a short time at intervals defined by the operator. Lumen diameters within each ROI can be measured independently of each other and accordingly shear stress can be calculated in the different ROIs, *i.e*. over different segments of the vessel.

Optimizing the different steps of the method was necessary to achieve a reliable high precision estimation of the internal luminal diameter. The following steps needed a strict evaluation and synchronization: FITC-dextran concentration, variability over time, background light, gain control regulation, shutter speed, calibration routines.

Transmission and Scanning electron microscope

Morphological validations of the vessel wall in umbilical arteries as well as the integrity of the endothelial monolayer of the artificial vessels were performed. These validation experiments were performed in separate series and are not reported in Paper I. At the end of the perfusion period (8 h for umbilical arteries, up to 48 h for the artificial vessels) the vessels were perfused with 5 mL 2.5% glutaraldehyde. For each vessel 10 min were allowed for fixation with vessels still connected to the perfusion system. Thereafter, the vessels were disconnected and placed in a formaldehyde reservoir. Vessels that had not been run in the perfusion system were fixed with formaldehyde and used as control. Randomly selected small pieces were prepared for morphological examination with transmission (LEO 912 AB Omega) and scanning (LEO 982 Gemini field emission SEM) electron microscopy (TEM and SEM, respectively).

For TEM examination post fixation was done with 1% OsO_4 and 1% potassium ferro cyanide in 0.1 M cacodylate for 2 h at 4°C, followed by a bloc staining with 1% uranyl acetate in H_2O for 1 h. Thereafter the vessels and tubes were dehydrated in a graded series of EtOH and infiltrated with epoxy resin (Agar 100, Agar Scientific LTD., Stanstead, UK), followed by curing by heat. Ultra thin sections (50-60 nm) were cut using a Reichert ultra microtome equipped with a diamond knife. Sections were collected on copper grids and counter stained with lead citrate and uranyl acetate before TEM examination. For SEM examination fixed vessels were dehydrated in ascending EtOH series and embedded in paraffin. The silicone scaffold was gently removed before they were deparaffinized in xylene and once again dehydrated in EtOH followed by immersion in hexamethyldisilazane and evaporated in a fume hood. The dried specimens were mounted on stubs. Digital images were taken with a Megaview III camera (SIS, Munster, Germany).

In the umbilical arteries the TEM and SEM images revealed an intact vessel wall as well as an intact endothelial layer. There were no signs of overhydration. No significant differences could be detected between the perfused and the control arteries (Figure 4 A and B).

In the artificial vessels an intact monolayer of endothelial cells could be detected by TEM and SEM images. However, due to preparation difficulties (swelling of the silicone) the SEM images revealed endothelial cells drifted apart from each other meanwhile the TEM images revealed intact tight junction between the endothelial cells (Figure 4 C and D).

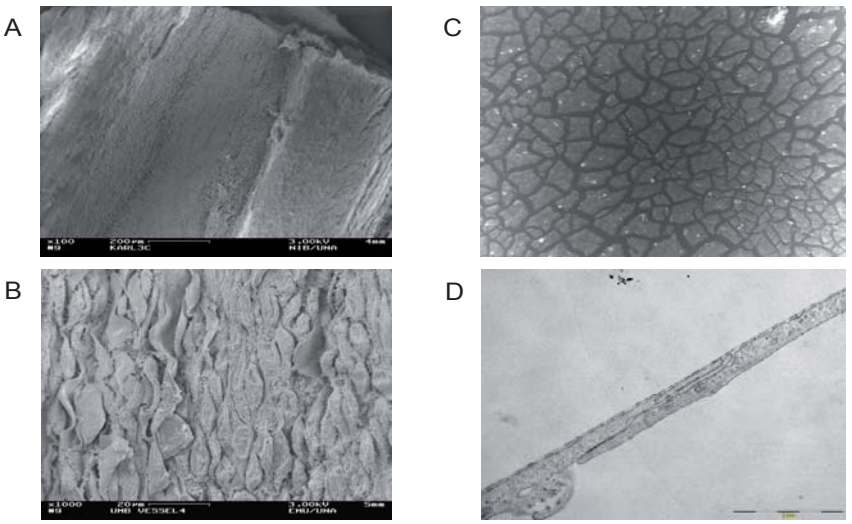

Figure 4. Validation of endothelial integrity with scanning and transmission electron microscopy. Figure A and B show images of the vessel lumen of an intact umbilical artery. Figure C is a scanning image of the endothelial cell layer in a silicone tube, where the cells are drifted apart due to preparation difficulties. Figure D is a transmission image of the endothelial cell layer showing intact tight junctions.

Software measurement and regulation

The perfusion system is monitored and regulated by a PC/Windows based software. The software was developed using LabVIEW 6.01 (National Instruments) and MatLab (Math Works). In the monitoring module the pressure and flow signals are continuously acquired. Further, in order to continuously evaluate the vessel diameter, a video image of the vessel is sampled. The control of pressure (upstream, downstream and intraluminal), volume flow, flow direction, shear stress, CO_2, and O_2 is regulated by a set of different electromagnetic valves and roller pumps. All monitor and regulating signals are subjected to calibration prior to start of an experiment (Figure 5).

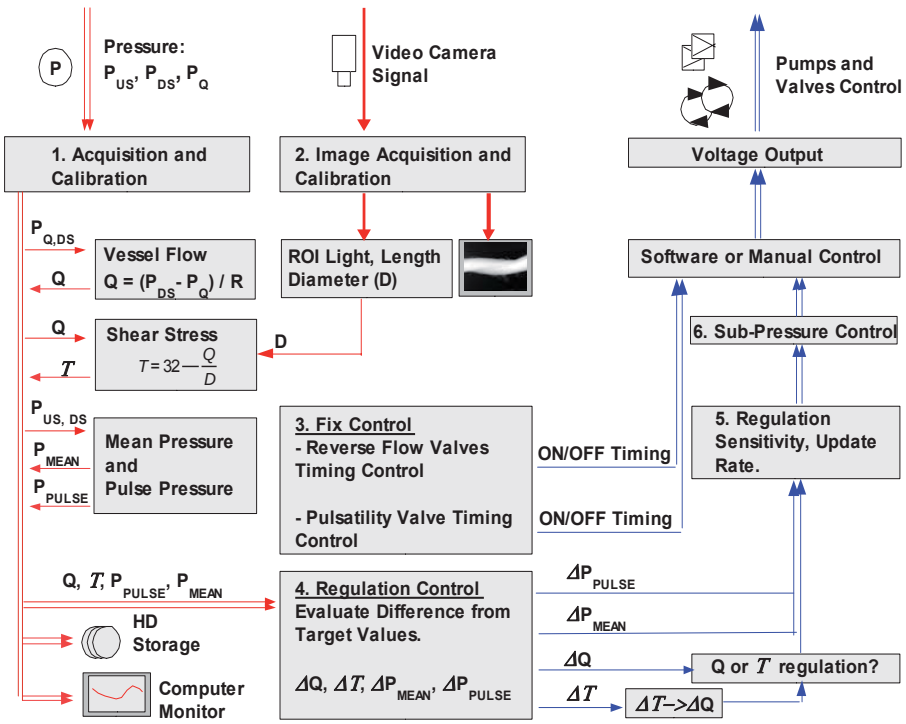

Figure 5. Schematic overview of software interfaces and functionality. Temperature, pH and pO_2 monitoring and regulation is excluded in the figure

Visualization and measurement of vessel

The algorithm is based on the assumption that the amount of light emitted from the FITC-dextran is proportional to the intraluminal vessel volume. The algorithm is calibrated prior to the start of the perfusion system. The intricate calibration procedure is based on an online image processing involving image filter, edge-detection and a dynamically compensation for changes of FITC-dextran concentration and light response sensitivity. The detection of the vessel edges involves a x- and y-edge-detec-

tion algorithm, based on a first derivative equation. The derivation of the image is performed using a 2-dimensional slope template used to convolve the image matrix. These derivatives are combined forming a gradient vector, one for each pixel. By using a linear fit model, the gradient vectors are "connected", thus detecting the edges of the vessel within each ROI defined by the operator. Once having the edges detected, a vessel length within the ROI can be calculated. Thereafter, in order to be able to measure the inner diameter of the vessel over a pre-specified ROI, a light/volume response factor has to be settled. It is done by using a specified pump-volume setting and a N_2-bubble transport time over the ROI. A reference capillary is used to compensate for time dependent FITC-dextran concentration/light response variations. With the assumption that the vessel intersection within a ROI is circular, the lumen diameter can be calculated using the measured volume value and the length of the vessel within the actual ROI. The reference capillary is constantly monitored and the change of the amount of light is used for online calibration of the volume-light response factor.

It was difficult to automatize the diameter calculation process and to create the operation to run online throughout an experimental setup. A MatLab algorithm was developed for this, called by the LabVIEW code, each time a new video image was acquired. This method required a lot of optimization before the precision of the method was acceptable. The following parameters were of special interest: efficient trade-off between performance and execution speed, image matrix size, acquisition speed and derivative convolution template size.

Regulation of biodynamic and metabolic parameters

The control loop of the regulation of the process variables, *i.e*. volume flow, shear stress, CO_2 and O_2 involves a "sensitivity problem". The regulation signals (control of pumps/valves) for a difference between the measured process variable and its desired set point have to be finely tuned.

These sensitivities, and corresponding response delays, may change from setup to setup, alter over time, pump flow *etc*. Several approaches were tested in order to find the most appropriate strategy. In the final version the software constantly compares the change of the regulator signal to the actual change of the process variable, thus evaluating a dynamically changing sensitivity factor in a kind of adaptive fashion.

A challenge was how to handle the fact that there may be a considerable time delay between a regulator signal change and the actual change of the process variable. In early versions this caused a lot of problems in terms of regulating oscillations and/or poor/slow regulation. A set of standard linear regulation algorithms based on PID-regulation concept was evaluated to handle this. Finally, the method chosen is a non-linear regulation algorithm using a forecast method. The regulator signal is controlled according to the difference of an estimated process variable value and the desired set point value. The estimation is done using the current process variable value, its derivative and the predicted response of the recently applied regulator signal changes. The forecast period may be changed by the operator, but is typically in the range of 20-120 s.

Pressure application

A special problem arose with flow profiles targeting low pressure with a moderate to high volume flow. As the downstream components (Luer connections, valves *etc.*) gave rise to a pressure drop, the pressure in the vessel was biased by that pressure drop. Even though the valves were wide open the pressure did not settle at all, or at least not fast enough. A set of solutions based on different connectors, valves *etc*. were tested without satisfactorily results. Instead of trying to minimize the flow resistance in the downstream flow circuits, a shift of the downstream pressure operation level was created. A variable sub pressure (*i.e.* negative pressure) was generated downstream of the vessel and downstream of all connections and valves. Hence, the generation of the sub pressure compensated fully for the pressure drop in the flow circuits.

Pulsatile flow and pressure

To create a device for the generation of physiological pressure/flow profiles was complicated. At first, a lot of effort was focused on the regulation of an electrically operated syringe. Even though it seemed to work in generating a wide range of different pulsatile pressure/flow profiles it was not possible to reach a sufficient precision level. Finally, a simple, yet powerful construction was created, composed of flow resistance in parallel with an open/close valve and a series of capacitances which generated a pressure/flow profile with acceptable regulating precision. The regulation of the opening and closing of the valve was controlled by the software to mimic the systolic and diastolic phases respectively.

By using the above monitoring and regulation facilities, pressure, pressure/flow profiles and direction, CO_2, O_2, flow and/or shear stress can be monitored and controlled by the software with high precision. It was complicated to construct software holding all complex calibrations, setups, user interactions, monitoring function, data storage and so forth. The software is run on an ordinarie PC with Windows OS and LabVIEW. Data is acquired by a modest sampling rate of 25 Hz and the regulation signals are updated by 100 Hz. The video image data is acquired in slightly lower pace and made time-coherent, using interpolation, with the other sampled signals. This is due to the fact that it is an extremely time-consuming process to handle each video image. A limitation of the system setup now is that evaluating the changes of the vessel diameter with good time resolution within each “heart beat” is not possible. This will required further optimization and development.

Mathematical background

Diameter: Assuming a circular cross-section of a vessel segment with length (l; cm) and intraluminal volume (V; ml), the diameter (d; cm), can be expressed as:

$$d = 2\sqrt{\frac{V}{l \cdot \pi}}$$

The volume can be expressed from the quantification of light emitted from the vessel segment (I) using a calibration factor (C_{IV}; ml), which may change over time:

$$V = I \cdot C_{IV}$$

The calibration factor's initial value is determined and set prior to start of perfusion. It is done by a low predefined volume flow (Q_{calib}; ml/min), the amount of emitted light (I_{calib}) over the vessel segment, and the passage time (t_{pass}; min) for a N_2 bubble to pass through the vessel segment. In order to compensate for FITC degradation, FITC concentration or light recording efficiency a reference glass capillary is continuously monitored ($I_{Ref}(t)$) and compared with the value at the calibration moment ($I_{Refcalib}$). Thus, the calibration factor is continuously tuned:

$$C_{IV} = \frac{Q_{calib} \cdot t_{pass}}{I_{calib}} \bullet \frac{I_{Refcalib}}{I_{Ref}(t)}$$

The calibration step is performed by a special module in the software.

The attenuation and scatter of the emitted fluorescence light through the vessel wall can vary between different vessels. This is corrected for by the calibration procedure which is performed at the beginning of each experiment on all vessels within each ROI. Any irregularity of light attenuation and dispersion does not have any impact on the diameter calibration.

Shear stress: Based on the vessel volume flow (Q; ml/min), the vessel diameter (d; cm), and the viscosity (η; g cm^{-1} s^{-1}) the wall shear stress (τ; dyn/cm^2) can be expressed as:

$$\tau = \frac{32 \cdot \eta \cdot Q}{\pi \cdot d^3}$$

Critical entrance length: The critical entrance length (L_e), *i.e.* the distance required until a fully developed laminar flow profile is established, can be approximated according to Hornbeck:

$$L_e = \frac{1}{300} \cdot \frac{\rho \cdot Q}{\pi \cdot \eta}$$

where Q is volume flow (ml/min), ρ is the density (g/cm^3) and η is the viscosity (g cm^{-1} s^{-1})

Reynolds's number: Reynolds's number (Re) is used to estimate potential turbulence within the flow system and can be described in a cylindrical tube as:

$$Re = \frac{\rho \cdot \frac{4Q}{\pi \cdot d}}{\eta}$$

where Q is volume flow (ml/min), ρ is the density (g/cm^3), η is the viscosity (g cm^{-1} s^{-1}) and d is the vessel diameter (cm).

EXPERIMENTAL AND ASSAY TECHNIQUES

Cell culture

Fresh intact umbilical arteries were used in Paper I. The tubes and glass capillaries used in Paper II-IV were seeded with a human umbilical vein endothelial cell (HUVEC) layer. In Paper III both HUVECs and human aortic endothelial cells (HAEC), (Clonetics, Cambridge) were used. Umbilical arteries and HUVECs were isolated from fresh umbilical cords obtained from normal deliveries at the maternity ward at Sahlgrenska University Hospital/Östra, Gothenburg, Sweden. The umbilical arteries were isolated by gentle dissection of the surrounding Wharton's jelly under sterile conditions. HUVECs were isolated by collagenase (Sigma-Aldrich) digestion [110]. In brief, the vein was mounted onto specially designed glass connections under sterile conditions and was infused by warm phosphate buffer saline (PBS) to remove the remaining blood. Thereafter, the vein was filled with 0.1% collagenase followed by gentle mechanical manipulation of the umbilical cord to explant the endothelial cells. HUVECs and HAECs were grown in plastic culture flasks in EGM-2 complete culture medium, consisting of EBM-2 basal medium (Clonetics) supplemented with 2% fetal bovine serum and growth factors (SingleQuots® kit; Clonetics) at 37°C in a humidified 5% CO_2 incubator. The cell culture medium was replaced every 2-3 days and subcultures were obtained by trypsin/EDTA treatment of confluent monolayers. In all experiments HUVECs were used in passage 1 and HAECs in passage 5.

Capillary microslides

For the shear stress studies (Paper II-IV) rectangular glass capillaries with internal length (L), width (W) and depth (D) = 10 x 0.4 x 0.04 cm (Microslides, Camlab, Cambridge, UK) were used [111]. Wall shear stress in the microslides was calculated by the following formula $\tau=6\eta Q/(W^2D)$, were Q is the volume flow (ml/min) and η is the viscosity of the medium (dynes x s/cm^2).

Distensible tubing

For the tensile stretch or pulsatile tensile stretch studies, distensible silicone tubes were used, specially manufactured by Specialty Manufacturing, Saginaw, MI, USA (Paper II, IV). The tubes were composed of dimethyl silicone applied over a bovine gelatin-coated glass or highly polished (electropolished) stainless steel mandrels (radius/thickness ratio = 20, *i.e.*, for 4.0 mm radius, thickness was 0.2 mm, with 100 mm length). Manufacturing tolerance for wall thickness was within 0.05 mm, which could result in some minor variability in tube elasticity. The internal diameter and surface area did not vary (a 4 mm diameter tube was 12.7 cm^2 and yielded 4-8 µg of total RNA from cell lysate).

The tubes used had an incremental elastic modulus of 12.4 x 10^6 dyn/cm^2, commensurate with *in vivo* vessels of this size [112]. Thus, pulse pressures of 0-180 mmHg translate to 0-19% strain and the pulse strain was uniformly radially applied to the side wall and thus cells lining the tube. Wall shear stress (dyn/cm^2) in the tubes was

calculated by the following formula $\tau=32\eta Q/(\pi d^3)$, where Q is the volume flow (ml/s), η is the viscosity of the perfusion medium (dynes x s/cm^2), and d is the diameter of the tube (cm).

Microslide and tube preparation and cell seeding

The capillary microslides and the silicone tubes were connected to the perfusion system by Luer connections. The connection between the slides/tubes and the Luer device consisted of a silicone rubber adaptor. Thereafter, they were rinsed with glutaraldehyde and 70% EtOH and then autoclaved. Solutions of 0.01% fibronectin (Sigma-Aldrich) were injected into the microslides/tubes and were thereafter incubated for one hour at an atmosphere of 5% CO_2 and a temperature of 37ºC. After this, fluid was withdrawn and replaced by cell culture medium for one hour before cell seeding. The slides and tubes were thereafter instilled with a cell suspension (6 x 10^5 cells/ml) and incubated at an atmosphere of 5% CO_2 and a temperature of 37ºC. A slow rotation of 10 rpm was applied to achieve uniform seeding using a custom rotisserie apparatus. Cells were allowed to attach for four hours. The slides were mounted in a custom-designed perfusion system and were flowed at a low flow rate, 0.005 ml/min. This was not necessary for the tubes since the silicone was permeable for oxygen diffusion and the cell medium volume was sufficient for the cells to attach and grow. The cells were then left for another 18 h. The endothelial layer was evaluated with a light microscope, and when confluence was achieved they were mounted in the perfusion system.

Streamer™ shear stress device

In Paper III a commercially available parallel-plate flow system was used, the Streamer™ shear stress device (Flexcell). This system enables stimulation of cultured cells with fluid-induced laminar shear stress. One of the reasons for using the Streamer™ system was the possibility to retrieve enough cell material to enable studies of the signaling mechanism behind the t-PA suppression by shear stress detected in the *ex vivo* perfusion system. In the Streamer™ device cells were seeded on fibronectin coated (Roche Diagnostics) glass culture slides. The cells where grown to confluence and thereafter mounted into two different Streamer chambers with either low (1.5 dyn/cm^2) or high (25 dyn/cm^2) shear stress. The two chambers shared perfusion medium (50% EGM-2, 50% M199, 2% FBS). Medium was driven through the chambers by peristaltic roller pumps. Each loop had pulse dampener to ensure laminar flow. The Streamer chambers were placed in a 37°C humidified 5% CO_2 incubator. Control slides with endothelial cells grown on identical fibronectin coated glass culture slides under static conditions, were placed in the same cell culture incubator. The shear stress experiments lasted up to 48 h in Paper III.

Shear experiments with MAPK inhibition were performed according to an identical protocol as described above, except that cells were preincubated with inhibitors for 1 h prior to shear stress stimulation. Ten micromolar of SP600125 (Calbiochem), SB203580 (Biosource), and PD98059 (Biosource) were used to inhibit JNK, p38 MAPK and ERK1/2, respectively. Inhibitors were present during the whole experiment.

Real-Time RT-PCR

Total RNA was extracted using RNeasy Mini Kit (Qiagen, Paper III, IV) or E.Z.N.A. total RNA kit, (Omega Bio-Tek, Paper II). Contaminations of DNA were removed by treatment with DNase (Qiagen, Omega Bio-Tek, respectively). Total RNA concentration and purity were determined by absorbance measures at 260/280 nm wavelength and RNA quality was controlled on 1% agarose gels. Next RNA was reverse transcribed to cDNA using the GenAmp RNA PCR kit (Applied Biosystems).

Levels of t-PA, PAI-1, u-PA, TM, VCAM-1, eNOS and GAPDH mRNA were analyzed with real-time RT-PCR. The real-time RT-PCR were performed on an ABI Prism 7700 Sequence Detection System (Applied Biosystems), and normalized relative to the reference gene GAPDH. GAPDH is a constitutively expressed gene, and thus works as an internal control to correct for potential variation in RNA loading and cDNA synthesis. The principle of the real-time RT-PCR method is that a fluorescently labeled probe hybridizes to its target sequence during PCR, and the Taq polymerase cleaves the reporter dye from the non-extendable probe. The reporter dye is then released to the solution and the increase in dye emission is monitored in real-time. The threshold cycle (C_T) is defined as the cycle number at which the reporter fluorescence reaches a certain level. There is a linear relationship between C_T value and the log of the initial target copy number as shown by Higuchi *et al*. [113]. Relative quantification of gene expression was analyzed as a treatment-to-control expression ratio using the comparative C_T method (User Bulletin #2, Applied Biosystems). The relative expression value of the target gene is obtained by calculating the difference in threshold cycles for a target and a reference gene in a treated sample, and comparing it to that of a control sample.

Oligonucleotide primers and Taqman® probes for quantification of t-PA, PAI-1, eNOS and GAPDH mRNA were designed from the GenBank database using Primer Express version 1.5 (Applied Biosystems), whereas u-PA and TM mRNA were quantified with Taqman® Assays-on-Demand™ and VCAM-1 mRNA with Taqman® Assays-by-Design™ (Applied Biosystems). The oligonucleotide sequences are presented in Table 1. All the primer pairs were selected so that the amplicon spanned an exon junction to avoid amplification of genomic DNA. t-PA, PAI-1 and eNOS probes were dual-labeled with 5´-reporter dye FAM (6-carboxy-fluorescein) and 3´-quencher dye TAMRA (6-carboxy-tetramethyl-rhodamine), while TM, VCAM-1 and u-PA were single-labeled with 5´-reporter dye FAM, (Table 1). cDNA from 30 ng of total RNA, Taqman® Universal PCR Mastermix (Applied Biosystems), 10 pmol of each primer and 5 pmol probe (1.25 µL 20X Assays-by-Demand or 0.42 µL 60X Assays-by-Design mix for u-PA, TM and VCAM-1) were mixed for each reaction in a final volume of 25 µL. All samples were amplified in duplicate or triplicate.

Enzyme-linked immunosorbent assay (ELISA)

Total t-PA protein in cell culture medium from shear stress and static cell cultures were determined by ELISA (TintElize t-PA, Biopool International) (Paper III). Due to large perfusion volumes, all samples were concentrated 10 times by vacuum cen-

Table 1. Primers and probes used in real-time RT-PCR

Gene	Oligonucleotide sequence
t-PA	FP: 5′-GGC CTT GTC TCC TTT CTA TTC G-3′ RP: 5′-AGC GGC TGG ATG GGT ACA G-3′ PR: 5′-TGA CAT GAG CCT CCT TCA GCC GCT-3′
PAI-1	FP: 5′-GGC TG ACTT CAC GAG TCT TTC A-3′ RP: 5′-TTC ACT TTC TGC AGC GCC T-3′ PR: 5′-ACC AAG AGC CTC TCC ACG TCG CG-3′
eNOS	FP: 5′-CGC AGC GCC GTG AAG-3′ RP: 5′-ACC ACG TCA TACT CA TCC ATA CAC-3′ PR: 5′-CCT CGC TCA TGG GCA CGG TG-3′
VCAM-1	FP: 5′-GGA AGA AGC AGA AAG GAA GTG GAA T-3′ RP: 5′-GAC ACT CTC AGA AGG AAA AGC TGT A-3′ PR: 5′-CCA AGT TACT CC AAA AGA C-3′
GAPDH	FP: 5′-CCA CAT CGC TCA GAC ACC AT-3′ RP: 5′-CCA GGC GCC CAA TAC G-3′ PR: 5′-AAG GTG AAG GTC GGA GTC AAC GGA TTT G-3′
u-PA	Sequences not provided by Applied Biosystems. ID: Hs00170182_m1
TM	Sequences not provided by Applied Biosystems. ID: Hs00264920_s1

Abbreviations: FP:forward primer, RP: reverse primer, PR: probe

trifugation (Speed Vac® Plus SC210A; Savant) prior to analysis. The principle of this assay is that the samples, or a standard containing human recombinant protein are added to microtest wells that are coated with anti-t-PA. After t-PA has been allowed to bind to the antibodies, peroxidase-labeled anti t-PA is added. Peroxidase then converts the substrate to a yellow product that is directly proportional to the amount of protein present in the sample. All samples were assayed in duplicate. Intra-assay variation coefficients was <5%.

Western blotting

Western blotting was used to study the effect of shear stress on the activation of the NF-κB, ERK1/2, p38 MAPK and JNK pathways (Paper III). Stimulated HUVECs were harvested in Laemmli sample buffer (Bio-Rad) with 5% β-merkaptoethanol, sonicated and boiled before being applied to a 10% Tris-Glycine gel (Cambrex) and electrophoresed in 1 X running buffer (Bio-Rad). Resolved proteins were transferred by electroblotting onto Hybond-P polyvinylidene fluoride membranes (Amersham Biosciences) in transfer buffer (25 mmol/L Tris, 192 mmol/L glycine, 20% methanol and 0.01% SDS). To minimize nonspecific binding, membranes were placed in blocking solution (5% fat-free dried milk in tris-buffered saline with 0.05% Tween-20 (TBST)) for 1 h. Thereafter, membranes were incubated over night, 4°C, with pri-

mary antibodies (Cell Signalling Technology) directed against the phosphorylated or total forms of p65 (NF-κB subunit), ERK1/2, p38 MAPK and JNK, 1:1000 in TBST supplemented with 5% bovine albumin, and thereafter with secondary antibody (anti-rabbit IgG, horseradish peroxides linked, 1:2000) in blocking solution for 1 h at room temperature. Proteins were visualized using SuperSignal Chemiluminescent Substrate (Pierce Biotechnology).

Electrophoretic mobility shift assay (EMSA)

EMSA was used in Paper III to detect interactions between nuclear proteins and gene regulatory elements in the t-PA promoter. Five double-stranded oligomers, each designed to contain a t-PA promoter specific element of interest, and consensus oligonucleotides for NF-κB were used as EMSA probes. The t-PA specific elements were as follows; the recently described functional κB element found in the t-PA gene of human neuronal cells [114] (5'-agggccggggattsssagtcta-3'), the t-PA cyclic adenosine monophosphate (cAMP) response element (CRE-)like site [115] (5'-attcaatgacatcacggctgtg-3'), the t-PA shear stress responsive element (SSRE) [116] (5'-caaggtctggtctcagccagacat-3') and the t-PA GC boxes II and III [117] (5'-acacagaaacccgcccagccgg-3' and 5'-accgaccccacccccctgcctgg-3'). To identify specific proteins involved in DNA-binding, supershift experiments were performed using antibodies (Santa Cruz) against HUVEC t-PACRE binding proteins [115] ; CREB, ATF-2, c-jun and c-fos.

The preparation of nuclear extracts from HUVECs was performed as previously described [118] and protein concentrations were quantified with a fluorometer (FLUOstar Optima; BMG Lab Technologies) using Bio-Rad reagents. Labeling of the oligomers was carried out as described using T4 polynucleotide kinase and [γ-^{32}P]ATP [119]. Annealing was performed (excluded step for consensus oligonucleotide) by adding a molar excess of the complementary strand to the kinase treated, heat inactivated mixture, which was subsequently heated to 95°C, after which the samples were left to anneal during the cooling process. Probes were gel purified by electrophoresis and eluted overnight at 37°C in buffer containing 0.5 M ammonium acetate and 1 mM EDTA. Supernatant solutions containing the labeled oligomer were precipitated to approximately 1000 cps/μL as previously described [120]. The binding reactions were carried out in a volume of 10 μL containing 5 μg crude nuclear extract in 2 μL Osborne buffer D [118], 1 μg poly [d(I-C)] [polydeoxy(inosinate-cytidylate)], 3 μL SMK buffer (12 mM spermidine, 12 mM $MgCl_2$, and 200 mM KCL) and ^{32}P-labeled probe (4 μL; 100 cps diluted in buffer D) as described. The protein/probe complexes were seperated on a 5% native polyacrylamide gel, and visualized by autoradiography. In supershift experiments antibodies were added to binding reactions before complexes were loaded on the gel.

Statistics

Data are presented as mean and standard error of the mean. All comparisons were done on samples from the same experiment. Linear regression calculation and linear correlation coefficient r (Pearson's r) were used in Paper I. One-way ANOVA (analysis of variance) was used in Paper II. Paired student's t-test was used in Paper II-IV. A p-value <0.05 was considered significant.

PERFUSION SYSTEM VALIDATION AND BIOLOGICAL RESULTS

Study I

Validation of diameter calculation

The accuracy of the new method of measuring the lumen diameter was evaluated in two different experimental setups. In the first experiment the inner diameter of glass capillaries with precisely defined diameters were measured. Close correlations were observed between the true and observed values in the range of 0.8 – 3.0 mm (r=0.99).

Thereafter, the diameter of intact umbilical arteries were measured and compared with direct ultrasonographic measurement of the same vessel segment. The ultrasonographic images were processed by image analysis software with a maximum resolution of 0.001 mm. Again, when comparing the ultrasonographically measured diameters with the measured diameter based on the amount of emitted light, a close correlation between the two methods was observed (r=0.99) (Figure 6).

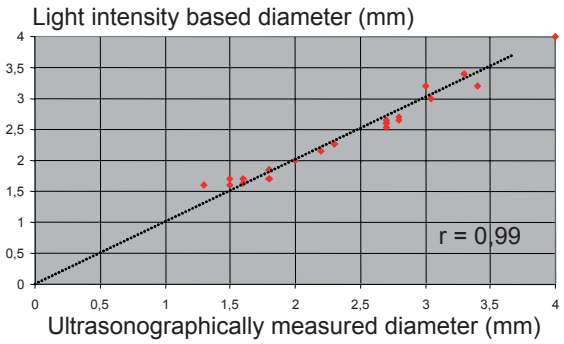

Figure 6. This diagram illustrates the correlation between light intensity based diameter measuring (y-axis) and ultrasonographically measured diameter (x-axis) of different vessels.

Validation of computer control and feedback algorithms

Control and feedback algorithms were challenged by switching between the different glass capillaries in a variety of combinations of constant shear stress (range 1-8 dyn/cm^2) and constant mean intraluminal pressure (range 20-120 mmHg). In these experimental setups the lumen diameter was instantaneously changed, which would not be the normal behavior of a biological living vessel.

The complexity of the system and its capacities is illustrated in Figure 7. The pulsation rate was predefined to 60 beats per minute, the systolic phase to 0.33 s, mean vessel pressure to 90 mmHg and mean volume flow to 40 ml/min. The pulse pressure was 120 mmHg; there was a diastolic pulse reflection and a short period of diastolic flow reversal. The maximum and minimum flow rates were 101 and -84 ml/min, respectively.

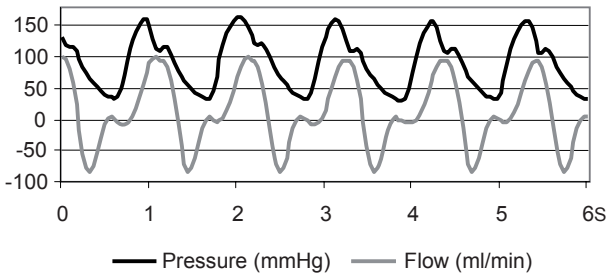

Figure 7. Illustration of a flow and pressure profile generated by the system.

The next system evaluation was performed on intact umbilical arteries. In these experiments, volume flow and mean intraluminal pressure were kept constant. The system was then challenged by varying the intraluminal diameter by adding various pharmacological substances. The endothelium-independent vasodilator sodium nitroprusside dehydrate was added to the perfusate to induce dilatation of the artery, and serotonin (5-HT) was used to induce vasoconstriction. As shown in Figure 8 A, sodium nitroprusside caused a dose-dependent vasodilation of the umbilical artery and serotonin caused a dose-dependent vasoconstriction. Thereafter, experiments were performed to evaluate endothelial function with the endothelium-dependent vasodilator histamine (Figure 8 B).

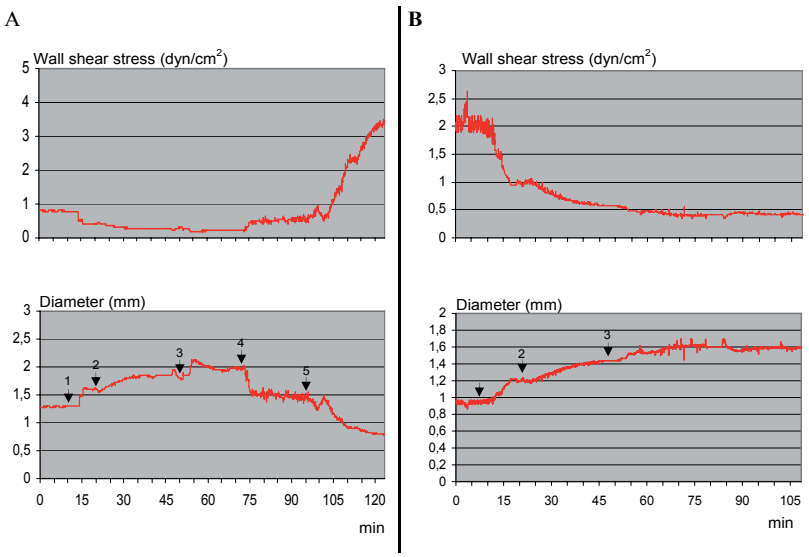

Figure 8. Pharmacological interventions in a perfused human umbilical artery. In these experiments mean intraluminal pressure and flow were kept constant. The dramatic changes in the vascular diameter induced by exogenously applied vasoactive substances caused large variation in shear stress since mean pressure and flow were kept constant. In Figure 8 A the following additions were made to the perfusate at a final concentration of (1) 6 x 10^{-5} M sodium nitroprusside dehydrate; (2) 4 x 10^{-4} M sodium nitroprusside dehydrate; (3) 10^{-3} M sodium nitroprusside; (4) 5 x 10^{-4} M 5-HT; (5) 10^{-3} M 5HT. In Figure 8 B the following additions to the perfusate were made at a final concentration of (1) 5 x 10^{-4} M histamine; (2) 10^{-3} M histamine; (3) 10^{-2} M histamine.

Study II

Shear stress suppressed expression of t-PA and VCAM-1

Prolonged unidirectional shear stress stimulation (24 h) of HUVECs resulted in a distinct dose-dependent reduction of t-PA and VCAM-1 gene expression (Figure 9). Compared to low shear stress, high and moderate shear stress resulted in a 49% ($p<0.001$) and 35% ($p<0.001$) reduction of t-PA gene expression, respectively. The reduction attained statistical significance even between high and moderate shear stress, $p<0.05$. High and moderate shear stress resulted in a reduction of VCAM-1 gene expression compared to low shear stress 70% ($p<0.001$) and 46% ($p<0.001$), respectively. Interestingly, shear stress regulation of VCAM-1 gene expression also seemed to be dose-dependent (moderate compared to high shear stress, $p<0.01$).

Shear stress induced expression of eNOS, TM, u-PA and PAI-1

Prolonged unidirectional shear stress stimulation (24 h) of HUVECs, resulted in a distinct increase of eNOS, TM and u-PA gene expression (Figure 9). This increase attained statistical significance in the high shear stress stimulated HUVECs as well as in the moderate shear stress stimulated HUVECs. High and moderate shear stress up-regulated eNOS gene expression compared to low shear stress, 4-fold ($p<0.001$) and 3-fold ($p<0.001$), respectively. High and moderate shear stress up-regulated TM gene expression compared to low shear stress, 5-fold ($p<0.01$) and 3-fold ($p<0.01$), respectively. The increase was dose-dependent, (moderate compared to high shear stress $p<0.05$). High and moderate shear stress up-regulated u-PA gene expression compared to low shear, 200% ($p<0.01$) and 160% ($p<0.001$), respectively. There was no difference between moderate and high shear stress, $p>0.05$. PAI-1 gene expression was only modestly increased by high shear stress, 32% up-regulation, ($p<0.05$), but not by moderate shear stress ($p>0.05$).

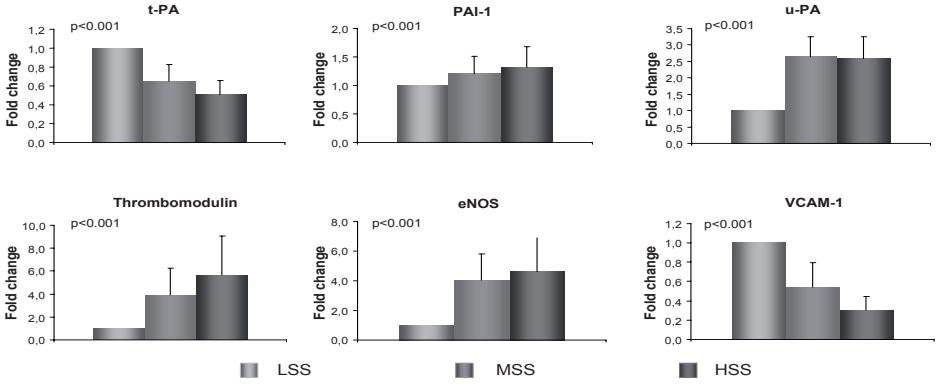

Figure 9. Effect of different shear stress levels on mRNA gene regulation of six different genes. Statistical comparisons are made relative to low shear stress (n=10).

Tensile stress had no gene regulatory effect on important hemostatic genes

In contrast to shear stress, tensile stress stimulation for 6 or 24 h of HUVECs displayed no regulatory effect on the six studied genes (t-PA, u-PA, PAI-1, TM, eNOS, VCAM-1) (Figure 10). There was no detectable effect, neither of different static intraluminal pressure levels (80 mmHg or 120 mmHg) nor of different pulsatile pressure levels (45 mmHg pulse pressure with a mean of 80 mmHg or 85 mmHg pulse pressure with a mean of 120 mmHg).

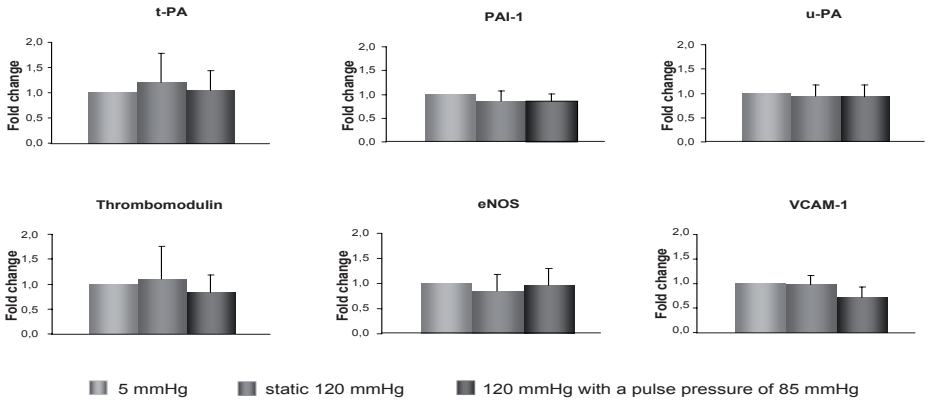

Figure 10. Effect of different static and pulsatile pressure levels on mRNA gene regulation of six different genes after 24h. Statistical comparisons are made relative to 5 mmHg (n=10).

Study III

Shear stress suppressed t-PA gene expression

To exclude the possibility that the shear stress suppressive effect on t-PA observed in Paper II was restricted to the specific experimental setup or to human umbilical vein endothelial cells similar experiments were performed with the Streamer^{TM} shear stress device (Flexcell) and tests were performed also on HAECs. These experiments confirmed the findings and showed an almost identical magnitude-dependent suppression of t-PA by high shear stress. Measurements of t-PA in the culture medium confirmed the observed shear effects also on the protein level. A magnitude-dependent suppression was observed after 24 h and 48 h. Furthermore, the shear stress suppressive effect was observed to be time dependent and the response could be confirmed in human aortic endothelial cells (Figure 11).

Shear stress mediated intracellular signaling

MAPK and NF-κB cascades have previously been suggested to be important pathways for intracellular signaling originating from mechanical forces which can lead to altered gene expression and protein synthesis [21]. Western blotting experiments directed against the activated (phosphorylated) forms of p65, ERK 1/2, JNK and p38

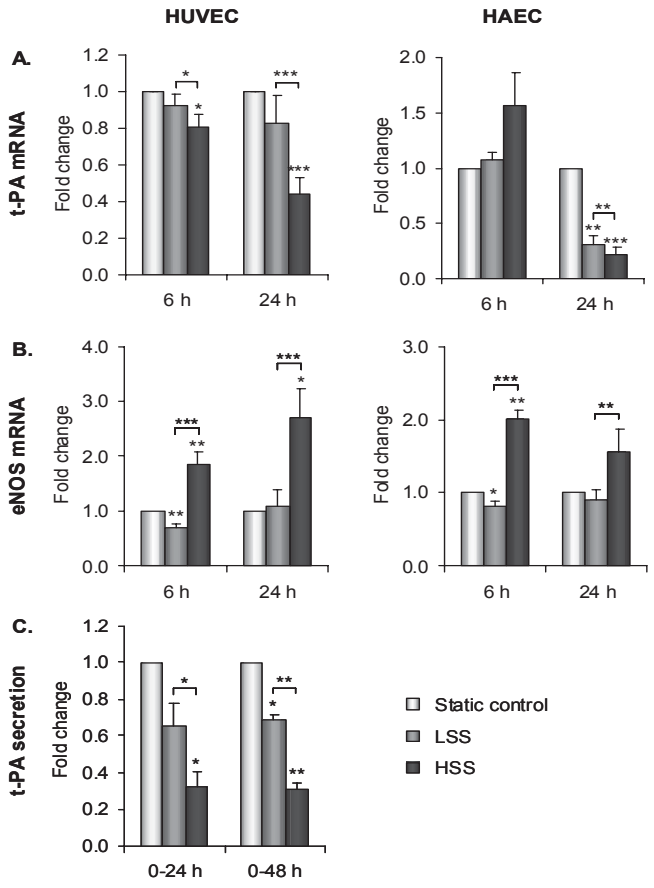

Figure 11. Effects of shear stress on t-PA and eNOS expression. Relative mRNA expression of (A) t-PA and (B) eNOS in HUVECs (n=8) and HAECs (n=6) exposed to LSS (1.5 dyn/cm2) or HSS (25 dyn/cm^2) for 6 or 24 h. (C) Relative t-PA secretion in HUVECs (n=3) exposed to LSS or HSS for up to 48 h. Unless indicated in the figure, statistical comparisons are made relative to static controls. *P< 0.05, **P< 0.01 and ***P< 0.001.

MAPK were performed. A rapid activation of all four studied signaling pathways by either low or high shear stress was observed after 1.5 h (Figure 12). However, the activation pattern was diversified with prolonged stimulation. NF-κB signaling, measured as phosphorylation of the p65 subunit, was relatively unchanged at 6 h, but gradually suppressed by increasing shear stress at 24 h. The initial increase in EKR1/2 activity was observed to level-off to basal levels by prolonged high shear stress stimulation. Meanwhile the elevated activity in low shear stress cells was preserved. Further, a similar pattern was observed for JNK signaling, where a relatively higher activity was observed in low shear stress stimulated cells after 24 h. Early low shear stress induced activation of p38 MAPK but was gradually decreased by prolonged stimulation, while high shear stress was observed to have a sustained high p38 MAPK activity.

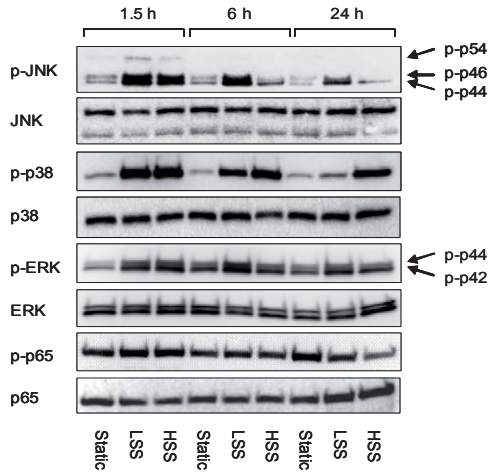

Figure 12. Effects of shear stress on phosphorylation of JNK, p38, ERK 1/2 and p65. Western blots showing JNK, p38, ERK 1/2 and p65 phosphorylation in HUVECs exposed to LSS (1.5 dyn/cm^2) or HSS (25 dyn/cm^2) for 1.5-24h. An unspecific signal is detected by the p-JNK antibody. As this signal is blocked by the ERK 1/2 specific inhibitor PD 98059 (10μM), it may represent p-p44 (data not shown). Data are representative of four independent experiments.

Shear stress modulated t-PA κB and CRE binding

EMSA experiments directed against five putative t-PA promoter specific sites were performed in order to determine the possible involvement of these sites in the shear stress induced suppression of t-PA. A marked induction of t-PA κB binding was observed after 3 h of low shear stress, while high shear stress showed a more modest induction. However, extended shear stress exposure for 24 h revealed no altered binding to this element. Also, t-PA CRE showed enhanced binding upon short-term shear stress exposure, n=10 (Figure 13). After 24 h, the pattern was reversed with most experiments showing a magnitude-dependent reduction in nuclear protein binding. Supershift experiments identified binding of c-jun and CREB, but not ATF-2 or c-fos. EMSA experiments directed against the t-PA SSRE, GC box II and GC box III elements showed no altered binding of nuclear proteins from either low or high shear stress HUVECs (3 and 24 h, n=4, data not shown)

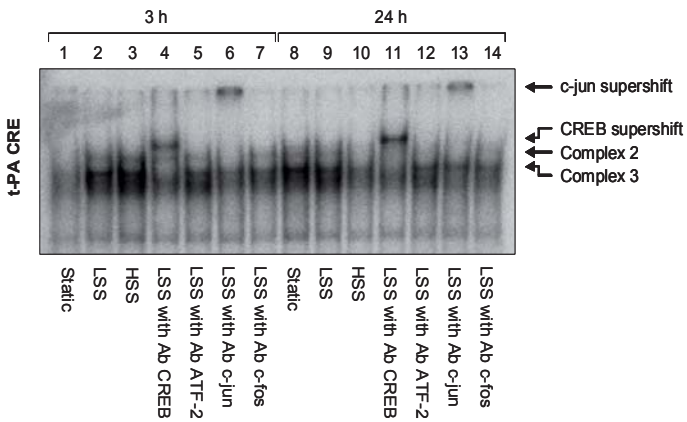

Figure 13. Effects of shear stress on nuclear protein binding to the t-PA specific CRE promoter element. EMSA on nuclear proteins from HUVECs exposed to LSS (1.5 dyn/cm^2) or HSS (25 dyn/cm^2) for 3 or 24 h. Lanes 4-7 and 11-14 with antibodies (Ab) directed against CRE binding proteins CREB, ATF-2, c-jun and c-fos. Arrows point out the shear-affected complex 2 and 3 and supershifts with c-jun and CREB antibodies. Data are representative of ten independent experiments.

Shear stress-induced suppression of t-PA was JNK-mediated

The EMSA results suggested that the t-PA CRE site was the most logical candidate for the t-PA shear stress response, and we proceeded by investigating potential upstream signaling mechanisms to this site. Shear stress experiments with pharmacologic inhibition of MAPKs were performed, as these pathways are known to affect t-PA CRE binding proteins.

Inhibition of JNK with 10 μM SP600125 showed an almost completely abolished shear stress response (Figure 14 A). The shear stress-induced suppression of t-PA was 13% and 66% with and without JNK (10 μM SP600125) inhibition, respectively ($p<0.01$), confirming our previous finding that JNK is a stimulatory pathway for t-PA expression [58]. Similar experiments with p38 MAPK (10 μM SB203580) and ERK1/2 (10 μM PD98059) inhibition indicated no involvement of these pathways, and the shear stress-mediated suppression of t-PA transcript was of an almost identical magnitude independently of p38 MAPK or ERK1/2 inhibition (Figure 14 B and C).

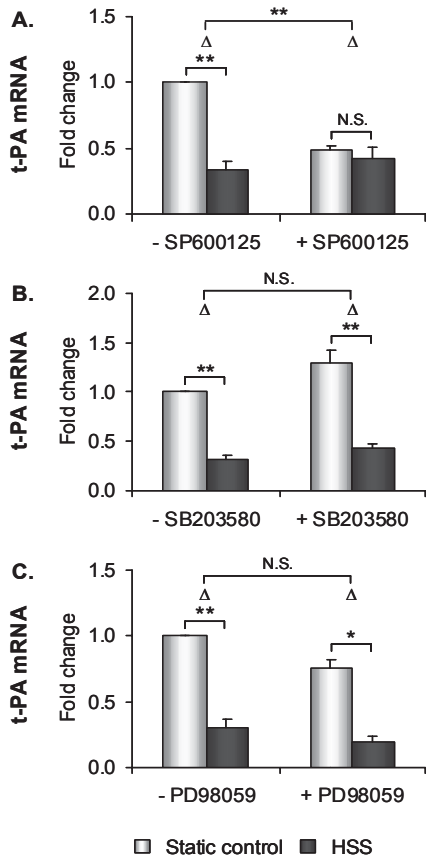

Figure 14. Effects of MAPK inhibitors on shear stress-mediated t-PA mRNA suppression. Relative mRNA expression of t-PA in HUVECs (n=3) preincubated with inhibitors against (A) JNK (10 μM SP600125), (B) p38 MAPK (10 μM SB203580), and (C) ERK 1/2 (10 μM PD98059) and thereafter exposed to HSS (25 dyn/cm^2) for 24h. *P<0.05 and **P<0.01.

Study IV

Shear stress modulated TNF-α gene regulatory effect

Again, shear stress showed a dose-dependent suppressive effect of t-PA gene expression (Figure 15 A). TNF-α in combination with low shear stress had a similar suppressive effect on t-PA, as high shear stress alone (LSS compared to HSS or LSS + TNF-α $p<0.001$, $p<0.001$, respectively, HSS compared to LSS + TNF-α: p=NS). However, our results indicated that moderate and high shear stress neutralized the suppressive effect observed by TNF-α (MSS compared to MSS and TNF-α p=0.8 and HSS compared to HSS + TNF-α p=0.35). Shear stress did not have a regulatory effect on u-PA gene expression (Figure 15 B). TNF-α had a modest 2-fold inducing effect on u-PA. Similar to t-PA, high shear stress seemed to block the effect of TNF-α on uPA (LSS compared to HSS + TNF-α, p=NS). Interestingly, TNF-α had a similar inducing effect on PAI-1 gene expression as moderate and high shear stress (approximately 50% induction each, $p<0.05$) (Figure 15 C). TNF-α in combination with moderate or high shear stress seemed to have an additive effect in inducing PAI-1 (LSS compared to MSS/HSS + TNF-α, 40% (p=0.012) / 56% (p=0.021), respectively).

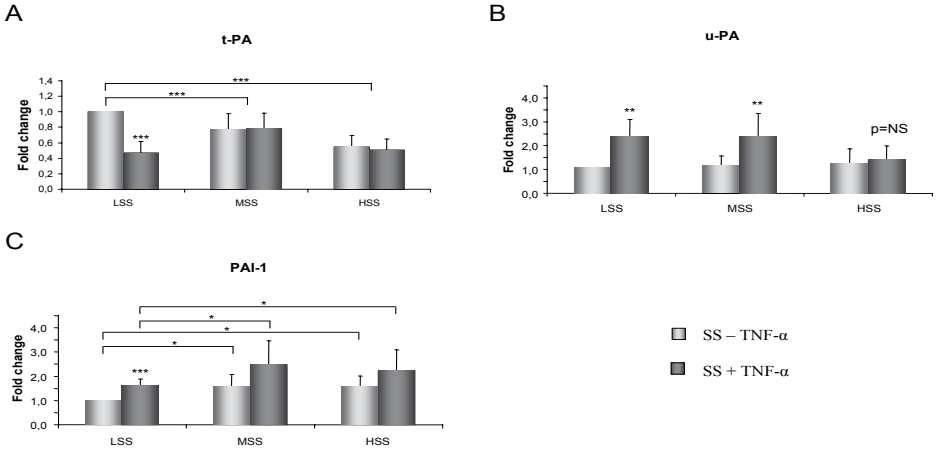

Figure 15. Relative mRNA expression of t-PA, u-PA and PAI-1 in HUVECs exposed to low (<1 dyn/cm^2), moderate (12.5 dyn/cm^2) or high (25 dyn/cm^2) shear stress with or without TNF-α for 24 h. Statistical comparisons are made relative to low shear stress without TNF-α (n=10). *P<0.05, **P<0.01 and ***P<0.001.

While shear stress had a strong inductive effect on TM gene expression (3-fold) (Figure 16 A), TNF-α and low shear stress had a strong suppressive effect on TM (7-fold). This suppressive effect was to some extent opposed by moderate and high shear stress (LSS + TNF-α compared to MSS/HSS + TNF-α, 3-fold (p=0.001) / 4-fold (p=0.005), respectively). However, TNF-α was the strongest stimuli. While shear stress had a 2-fold inducing effect on eNOS gene expression, TNF-α and low shear stress had a strong suppressive effect (5-fold) (Figure 16 B). This was to some extent opposed by moderate and high shear stress (LSS + TNF-α compared to MSS/HSS + TNF-α, 3-fold ($p<0.001$) / 4-fold (p=0.005), respectively). Shear stress had a dose response suppressive effect on VCAM-1 (Figure 16 C). TNF-α massively induced VCAM-1

while increasing levels of shear stress to some extent could counteract this induction (LSS + TNF-α compared to MSS/HSS + TNF-α, 45% ($p<0.05$) / 65% ($p=0.01$), respectively).

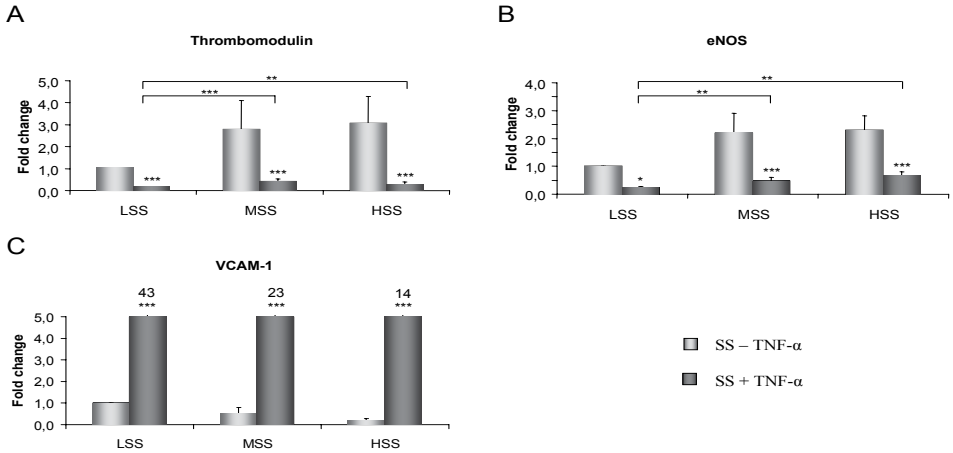

Figure 16. Relative mRNA expression of thrombomodulin, eNOS and VCAM-1 in HUVECs exposed to low (<1 dyn/cm^2), moderate (12.5 dyn/cm^2) or high (25 dyn/cm^2) shear stress with or without TNF-α for 24 h. Statistical comparisons are made relative to low shear stress without TNF-α (n=10). *P<0.05, **P<0.01 and ***P<0.001.

Tensile stress did not modulate TNF-α gene regulatory effect

Static or pulsatile tensile stress was shown in Paper II to lack a regulatory effect on t-PA, u-PA, PAI-1, TM, eNOS and VCAM-1. Meanwhile, TNF-α showed a stronger regulatory effect on the studied genes. It had a suppressive effect on t-PA, TM, eNOS and an inductive effect on PAI-1, VCAM-1 and u-PA. Inflammatory stress did not render the EC in a distinct phenotypic mode where they became sensitive to static or pulsatile tensile stress (Figure 17). Thus, tensile stress did not have a regulatory effects on the selected genes in a proinflammatory activated endothelium.

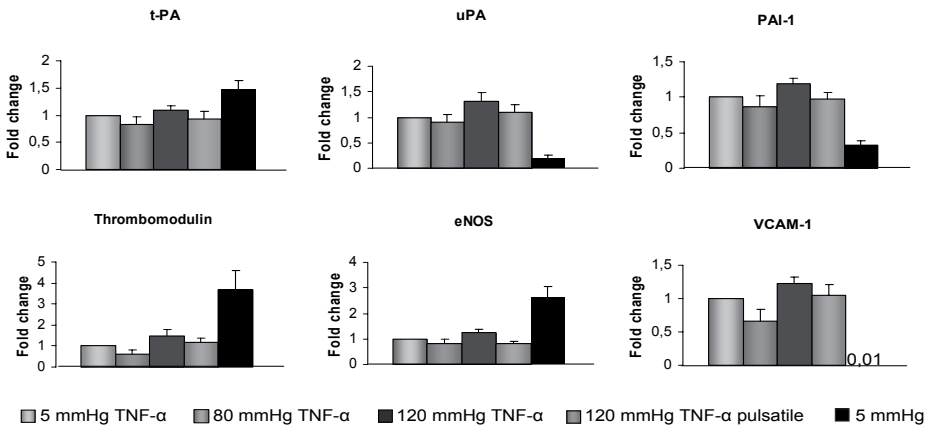

Figure 17. Relative mRNA expression of t-PA, u-PA, PAI-1, thrombomodulin, eNOS and VCAM-1 in HUVECs exposed to different levels of pulsatile/static tensile stress with or without TNF-α for 24h. Statistical comparisons are made relative to 5 mmHg with TNF-α (n=16).

DISCUSSION

Elucidation of the mechanisms of vascular adaptation due to changes in biomechanical flow conditions is an important issue in vascular biology under normal and diseased states. Many different systems have been designed to subject endothelial cells to mechanical stress. In most of these systems, one or a maximum of two mechanical forces can be applied at the same time. However, the physiological mechanical environment generated during the cardiac cycle has a more complex nature, which includes different combinations of shear stress, pressure and cyclic tensile stress. Therefore, more refined and advanced biological perfusion systems are needed that as accurately as possible mimics the *in vivo* conditions.

Development of a new *ex vivo* perfusion system

Most of the systems previously described can differentiate between pressure and flow [30, 121-123], but they cannot be used to simultaneously and differentially control shear stress and complex intraluminal pressure and flow profiles. Few systems admit determination of mean shear stress over the vessel segment [108, 109] and to our knowledge, no other system permits shear stress measurement at different discrete points of the vessel continuously.

The shortcomings of each approach have contributed to the relative paucity of studies on the vascular remodeling and adaptation process to different biomechanical stress combinations. This important gap prompted us to develop a perfusion system suitable for perfusion of intact living blood vessels or artificial vessels that mimic advanced physiological *in vivo* flow profiles. The major advantage of our system over prior models is the ability to combine virtually any of the biomechanical forces present, under normal as well as pathological states, under well-regulated conditions and online monitored. Importantly, shear stress can be measured at different segments of the vessel and the pulsatile wave form and oscillatory flow patterns can be varied in endless combinations.

Early attempts to perfuse intact vessels with irregular geometry and variable resistance under well-defined biomechanical conditions were hampered by the problems of defining and thereby controlling shear stress online. With traditional approaches it was challenging to calculate shear stress without monitoring vascular resistance [108] or direct lumen measuring [109] with high precision, and thereby difficult to adjust deviations from target levels continuously. In our new system, shear stress calculation is based on the intraluminal diameter which is measured by quantification of the light emission from a fluorescent perfusion medium in the vessel lumen, proportional to the lumen diameter. The molecular size of the FITC-dextran is large enough to prevent any leakage through the vessel wall, even in the presence of endothelial damage.

Furthermore, the system admits measurement of irregular lumen diameters and determination of shear stress at different loci, *e.g*. upstream and downstream of stenoses or other flow obstacles.

Given the critical dependence of adequacy of the inner diameter measurement for calculation of shear stress, it was necessary to perform careful physical and biological validations of the method. Excellent agreement was found between the true and observed diameter readings in the glass capillaries as well as in the vessels. Since calibration is done separately for each ROI, any difference in emitted light attenuation or dispersion does not have any effect on the correctness of the diameter measurement. The lumen measurement technique we use has two advantages compared to the technique used by VanBavel *et al*. [109]. First, by deploying a reference glass capillary, any variations in the light to volume factor (FITC concentration, mercury lamp *etc*.) is compensated for. Second, performing light-to-volume calibration precludes the necessity of visual lumen detection or measurement, which is a great advantage. Taken together with the exactness of the flow measurements by the high-precision flow meters, the present approach can provide very accurate and reliable measurements of shear stress.

An additional advantage of *ex vivo* systems similar to the one presented here is that it admits perfusion studies of intact biological vessels. Previous co-culture studies have demonstrated that cross-talk between vascular smooth muscle and the endothelium is important and can alter the nature of cellular signaling to mechanical stimulation [124-126]. Studies in whole animal models preserves the entire vessel integrity but interpretation is often complicated by difficulties in monitoring biomechanical stress profiles and controlling additional extrinsic variables, *e.g*. hormones and nervous regulation. Furthermore, cultured endothelial cells often undergo phenotypic changes that can influence mechanosignaling responses and complicate data interpretation. However, when an intact vessel is perfused, there is a potential risk for overhydration of the vessel in long term experiments. This is important since elastic modules and other biomechanical parameters may be altered. This overhydration varies considerably with different perfusion media, between arteries and veins, between vessels of different origin and also between vessels from different species. Since our perfusion system can detect and measure both the outer (light microscopy) and the inner (fluorescence microscopy) diameter of the vessel, the geometry of the vessel can be calculated before, during and after perfusion. Alterations in elastic properties due to swelling of the vessel wall can be analyzed by measuring diameter responses after application of various levels of intraluminal pressure.

The present setup, with the use of tubing pumps, limited us to use cell-free perfusion fluids. However, there are no limitations in altering the perfusion medium, *e.g.* in terms of shear dependent viscosity, by adding dextran or by using cell cultivation medium. An interesting further development of the model may be to exchange the tubing pumps with centrifugal pumps, which will make it suitable for studies with cell-containing perfusion media.

Influence of complex hemodynamic stress on hemostatic genes

Many of the previously reported systems combining pulse distension and flow have employed a sinusoidal waveform to generate pulsatility [30, 127]. This distinction

may be important because the physiological waveform yields nearly an order of magnitude greater rate of strain and shear change when compared to a sine wave of similar amplitude [112]. Indeed, there are observations indicating that rapidly changing flow, oscillatory flow with flow reversal and low net flow tend to induce a more pathologic state compared with laminar flow or oscillatory flow that remains unidirectional [30, 31, 33]. Higher pulse pressure, which is strongly related to stiffness of the arterial wall, is associated with endothelial dysfunction [34, 35]. In order to address these issues we performed experiments where endothelial cells were exposed to different levels of static pressure with or without pulsatile stress and at the same time controlling a steady laminar shear stress. In the next series, pressure was kept constant while shear stress levels were altered. Based on our interest profile we chose to study six key hemostatic genes (t-PA, u-PA, PAI-1, TM, eNOS and VCAM-1).

We found that shear stress was a much more powerful stimulus than static or pulsatile tensile stress. Shear stress suppressed, in a dose-response dependent manner, t-PA and VCAM-1, while TM was induced. u-PA, eNOS and PAI-1 were upregulated by shear stress, but there was no obvious dose-dependent effect on these genes. Pressure, static or pulsatile, under controlled flow, was not capable of significantly influencing mRNA expression of the six studied genes. There may, of course, be other genes in the endothelial cell that may respond to tensile stress but even microarray studies including thousands of genes have suggested that tensile stress compared to shear stress in general has a much weaker regulatory effect on endothelial gene expression pattern [128, 129].

We previously reported on cyclic stretch effects on t-PA, PAI-1 and u-PA in human aortic endothelial cells after 48 hours of stimulation [28]. However, these effects were of minor magnitude and in a stretch device without flow control. Frye *et al*. [130] reported in 2005 the risk with stimulation setups where not all hemodynamic forces are under control. They showed that different stretch devices, where cells are stretched over an elastic membrane, create an uncontrolled fluid motion of the medium. The influence of this motion of the medium, even though it was only a reversing shear stress of less than 0.5 dyn/cm^2, seemed to be the essential gene regulatory stress for most of the responsive genes studied. Once again, this illustrates the importance of more complex perfusion systems were the mechanical forces are combined and under strict control.

Within the vessel wall, physiologic stress is mostly manifested as cyclic strain, while in the lumen, the endothelial cells are mainly subjected to shear stress [21, 131]. The vascular wall responds to and compensates for changes in the local biomechanical flow environment almost immediately via endothelial mediated dilation or smooth muscle contraction. In the case of hypertension, vascular remodeling will occur in the long term with media thickening and narrowing of the lumen. This may impair the important endothelial shear stress dependent regulatory system [132, 133]. Khayutin *et al*., proposed that it was physiologically more relevant for endothelial cells to be sensitive to shear stress and not to tensile stress, since mean intraluminal pressure varies considerably over time while shear stress is more or less constant [133]. This

is well in line with our observations of no regulatory effect on the six marker genes neither after 6 nor 24 hours of pulsatile pressure stimulation.

One drawback with this system is that it has limited capacity to provide specific information on mechanisms of gene regulation. Studies with pulsatile stimulation at high shear levels are complicated since the accuracy of the formulas that can be used to approximate pulse-flow shear stress are dependent on the elastic properties of the vessel. The strength, on the other hand, is the possibility to elucidate complex gene expression patterns, which can be further focused on detail in more suitable systems.

Shear stress suppressive effect of fibrinolytic gene expression

Surprisingly, we found that laminar shear stress had a suppressive effect on t-PA mRNA and protein. This suppressive effect, observed in our *ex vivo* perfusion system, was also confirmed in the commercially available Streamer^{TM} shear device (Flexcell, Hillsborough, NC, USA). Even though shear stress has been extensively studied, reports on t-PA and its regulation are scarse. Previous reports have suggested that shear stress induces t-PA protein secretion [24, 59]. Based on semi-quantitative Northern blotting techniques, t-PA gene expression has also been shown to be induced by shear stress [59, 134, 135], but one of the laboratories was unable to reproduce these data in a more recent study based on the microarray technique [128]. In a previous study from our group we found that the capacity for acute release of t-PA is markedly impaired in patients with hypertension [136] and that this can be restored by lowering of blood pressure [137]. Hypertension is associated with vascular wall remodeling causing shear stress alteration, which could in part explain the suppression of t-PA. Recently, our *in vitro* results were also confirmed by Metallo *et al*. who reported on a similar suppression of t-PA by shear stress in different endothelial cell types [138]. The validity of the responses in our systems was also strengthened by confirming previous documentation on shear-dependent eNOS and VCAM-1 regulation [53, 55].

Mechanical forces have been suggested to signal through the MAPK and NF-κB cascades, and our group has previously shown that the JNK pathway induces t-PA gene expression whereas the p38 MAPK and NF-κB pathways mediate suppression [58]. Interestingly, western blotting of shear stress samples showed reduced JNK and enhanced p38 MAPK activity. Further, inhibition experiments demonstrated no involvement of the p38 MAPK pathway but a critical dependence on JNK signaling. Since JNK inhibition reduces basal t-PA expression, our data indicate that the shear stress-induced suppression of t-PA is mediated by reduced JNK signaling, an effect of shear that is in line with previous reports [139]. The observation that long-term shear stress experiments showed a reduced binding of c-jun and CREB to the t-PA CRE site may indicate that the t-PA response involves this element, which is known to bind effector molecules of the JNK pathway [115]. However, in contrast to inflammatory stimulation, shear stress-induced suppression of t-PA does not seem to involve NF-κB signaling. We observed a declining NF-κB activity and unaltered binding to either the t-PA κB site or a consensus NF-κB element upon long-term shear stress exposure. Similar effects on NF-κB activity has been reported in HAECs, where high shear stress induced a rapid transient activation which reversed and declined upon continued exposure [140].

Thus, although laminar shear stress of physiologic levels has been shown to convey some atheroprotective effects on the vascular wall and retard atheroma formation [141], the present findings of suppressed t-PA expression, but also induced PAI-1 expression, indicate that such positive effects of shear stress do not necessarily extend to those exerted on the fibrinolytic system.

Influence of TNF-α and biomechanical stress on hemostatic genes

Hypertension, acute/chronic coronary syndrome, intermittent claudication *etc*. are clinical states most often associated with a low grade of inflammation and a disturbed biomechanical flow profile. Therefore, we found it important to study the combined effects of inflammatory and biomechanical stress. The cytokine TNF-α is an important mediator of the inflammatory process which causes endothelial dysfunction and promotes the atherosclerotic process. Different levels of tensile or shear stress in combination with TNF-α were studied in the perfusion system. Our findings indicate that moderate and high shear stress can modify the endothelial cell sensitivity to inflammatory stress while low shear stress and tensile stress can not.

To our surprise, static and pulsatile tensile stress seemed to lack gene regulatory effect on the studied genes in Paper II. However, previous studies have shown that genes non-responsive to TNF-α were shifted to a TNF-α sensitive state by biomechanical stress [52]. Therefore, we hypothesized that cytokine stimulation may cause ECs to become sensitive to different combinations of tensile stress. However, we could not observe such a mode shift in ECs by cytokine stimulation. None of the studied genes modulated their response to TNF-α by simultaneous tensile stress stimulation.

By contrast, shear stress was a potent stimulus. Moderate and high shear stress modulated the response to cytokines in all the studied genes. The effect of shear stress and TNF-α on VCAM-1 and eNOS are in accordance with previous reports [53, 55, 56]. The uniqueness of our study approach was that the effect of different shear stress levels in combination with TNF-α was addressed. The setup enabled a direct comparison of the effect of TNF-α with unstimulated ECs exposed to identical shear stress, which has been a shortage in previous reports. This is important in validating the intergroup significance for different stimulations *e.g*. thrombomodulin, eNOS and VCAM-1 in this study. Regarding thrombomodulin, the meaningfulness can easily be exaggerated of the 2-3 fold induction of shear stress on TNF-α stimulated ECs. However, when comparing it to non-inflamed shear stressed ECs, the relative quantitative effects are modest. Inflammatory stress was a quantitatively stronger stimulus than shear stress on thrombomodulin, eNOS and VCAM-1.

It is interesting that shear stress in combination with TNF-α can have bidirectional effects on different genes, *i.e*. shear stress attenuated cytokine-induced expression of VCAM-1 opposed the effects on thrombomodulin and eNOS gene expression and additively induced PAI-1 expression, whereas shear stress seemed to totally block the cytokine-suppressive and inducing effects on t-PA and u-PA, respectively. Shear stress showed a dose-dependent suppressive effect on t-PA. TNF-α in combination with low shear stress demonstrated a suppression of t-PA, similar to the effect of high

shear stress alone. However, our results indicate that moderate and high shear stress neutralize the suppressive effect observed by TNF-α. Shear stress did not seem to have any regulatory effects on u-PA gene expression, while a modest inducing effect was observed with TNF-α. As for t-PA, high shear stress seemed to induce a blocking effect of TNF-α on u-PA. Interestingly, TNF-α and low shear stress showed a similar inducing effect on PAI-1 mRNA as moderate and high shear stress. TNF-α in combination with moderate or high shear stress seemed to have additive effects in inducing PAI-1. Regarding thrombomodulin, shear stress counteracted the suppressive effect exerted by TNF-α on thrombomodulin gene expression.

CONCLUDING REMARKS

In the present work we have developed a system suitable for many studies, including intact biological vessels of different sizes as well as possible artificial vessels, or different perfusion chambers for cultivated cells. The advantage of this system compared to previous developed ones is that it permits stimulation of a wide range of biomechanical stress within the same system under controlled metabolic conditions. Previous system setups have been hampered by difficulties in monitoring and regulating the different types of biomechanical stress. The danger with these approaches is that the background "noise" may be of critical importance which was elegantly demonstrated by Frey *et al.* in a stretch device system [142]. It is also of importance when comparing different stimuli with each other that the experimental setups are as identical as possible except for the actual stimuli of interest. The present model overcomes many of these shortcomings and has the potential of expanding our understanding of a variety of vascular adaptations to alterations in local flow and pressure conditions.

Atherosclerotic plaques are not randomly located within the vascular tree. Interestingly the heterogeneity of the distribution of plaque is closely correlated with specific local hemodynamic flow profiles, characterized by low shear stress, turbulence, flow reversal and oscillatory flow. Furthermore, biomechanical stress has also been shown to regulate a number of physiological functions in the vessel wall, *inter alia* vascular tone by release of vasoactive substances, vascular adaptation and remodeling by growth factors, formation of new blood vessels and the vessel's thromboprotective mechanisms. It was of great surprise that tensile stress did not have any regulatory effect on six important marker genes, representing different hemostatic functions, while shear stress was a powerful stimulus.

Low grade inflammatory activity has emerged as an important determinator of vascular dysfunction and progression of atherosclerosis as well as endothelial dysfunction. It has been suggested that shear stress has the capacity to protect the endothelium from some of the negative effects of inflammatory stress. The interaction between tensile and inflammatory stress has not previously been studied. In the present studies we found that shear stress but not tensile stress was able to strongly interfere with the inflammatory response in a protective way.

A possible pathophysiological scenario is that the local hemodynamic forces lead to a lower threshold for the induction of genes related to endothelial dysfunction in lesion-prone areas upon negative stress. Disturbed flow with low shear stress and high shear gradients may predispose these regions to the early events of atherosclerosis and thrombosis. These areas are rendered more vulnerable to negative systemic stimuli, such as inflammatory stress. In contrast, the endothelium in the lesion-resistant areas may be desensitized to noxious stimuli by the laminar flow with high shear stress. In conclusion, imbalanced expression of hemostatic genes by the endothelium ("endothelial dysfunction") constitutes an important pathogenetic risk factor for vascular diseases such as atherosclerosis. Increasing understanding of these intricate relationships is crucial in finding new therapeutic strategies to prevent cardiovascular mortality.

CONCLUSION

An *ex vivo* perfusion system was developed permitting virtually any combination of the biomechanical forces present under normal as well as pathological states under well-regulated conditions and online monitored.

Shear stress but not tensile stress had a powerful gene regulatory effect on mRNA expression of t-PA, u-PA, PAI-1, TM, eNOS and VCAM-1.

Laminar shear stress magnitude dependently suppressed t-PA gene expression by a JNK dependent mechanism.

Physiological levels of shear stress but not tensile stress modulated the inflammatory response as well as anti- and pro-thrombotic functions in endothelial cells stimulated by TNF-α.

POPULÄRVETENSKAPLIG SAMMANFATTNING

Hjärt-kärlsjukdomar är en av de vanligaste dödsorsakerna i den industrialiserade världen. Ruptur av åderförkalkningsplack leder till aktivering av koagulationskaskaden som ohämmat bildar en kärltilltäppande tromb, vilket resulterar i hjärtinfarkt och slaganfall. Trots att hela kärlträdet exponeras för systemiska riskfaktorer, finner man åderförkalkningsplack företrädesvis i kärlförgreningar där flödesprofilen ofta är ogynnsam. Blodkärlets vägg har ett eget inneboende försvarssystem mot blodproppsbildning - fibrinolysen. Experimentella studier har visat att den lokala biomekaniska flödesprofilen och låggradig inflammatorisk stress påverkar kärlväggens funktion. Avhandlingsarbetets syfte var att utveckla ett perfusionssystem för att kunna studera hur biomekanisk och inflammatorisk stress påverkar den vaskulära hemostasen.

I **delarbete I** utvecklades och utvärderades ett datorstyrt perfusionssystem som möjliggör perfusion av intakta såväl som ”artificiella” blodkärl under strikt kontrollerade flöde och metabola förhållanden. Styrkan med detta nya modellsystem är att de olika kraftkomponenterna som cellerna påverkas av i kroppen kan separeras och studeras var för sig eller i olika kombinationer. Systemet kan generera pulsatila tryckkurvor som efterliknar förhållandet i kroppen, systoliska respektive diastoliska fasen kan kontrolleras och utformas på olika sätt. Systemet möjliggör även att mäta innerdiametern av kärlet inom olika segment. Detta är en styrka vilket medför exakta beräkningar av skruvningskraften istället för att denna estimeras, vilket är fallet i de flesta tidigare liknande modellsystem. Styrkan och det unika med detta system är att olika kombinationer av mekaniska krafter kan studeras i ett och samma perfusionssystem under väl reglerade förhållanden.

I **delarbete II** gjordes en biologisk utvärdering av systemet samt en utvärdering av olika krafters inverkan (olika nivåer av statisk och pulsatile sträckning eller olika nivåer av skuvningskraften) på reglering av 6 viktiga hemostasgener (t-PA, PAI-1, u-PA, TM, eNOS och VCAM-1). I detta arbete odlades humana endotelceller från navelstängsvenen (HUVEC) i silikonslangar alt glaskapillärer, därefter perfunderades de under 6 respektive 24 timmar. Till vår förvåning verkade endast skuvningskraften ha en dosrespons reglerande effekt på mRNA nivå på de gener vi valde att studera. Skuvningskraften nedreglerade t-PA och VCAM-1 medan u-PA, PAI-1, TM och eNOS uppreglerades.

I **delarbete III** gick vi vidare med fyndet från delarbete två att skuvningskraften nedreglerar t-PA. Detta skiljer sig från ett fåtal tidigare publicerade artiklar som påvisat en uppreglering av t-PA av skuvningskraften. Initialt för att bekräfta resultaten gjordes liknande försök i ett annat modellsystem (Streamer^{TM}) med HUVEC såväl som humana aorta endotelceller, (HAEC). Vi kunde även här se en dosberoende nedreglering av t-PA på mRNA och protein nivå. Vi kartlade de intracellulära signaleringsvägar genom vilka skuvningskraften skulle kunna inhibera t-PA expressionen. Detta utfördes genom att tillsätta olika inhibitoriska substanser som blockerar kända signaleringsvägar (MAPK, NF-κB). Våra slutsatser från detta arbete är att t-PA produktionen blockeras av skuvningskraften via hämning av MAP-kinaset JNK.

Delarbete IV är en studie av hur inflammatorisk stress, medierad via TNF-α, påverkar endotelceller som samtidigt utsätts för olika kombinationer av mekanisk stress. Vår grupp har i ett tidigare arbete kartlagt hur t-PA påverkas av TNF-α i statiskt odlade endotelceller. Varken statisk eller pulsatile tensil stress kunde påverka endotelcellernas respons på inflammation. Däremot kunde shear stress modulera den inflammatoriska stressen på samtliga studerade gener (t-PA, u-PA, PAI-1, TM, eNOS och VCAM-1) på mRNA nivå.

Sammanfattningsvis har ett helt nytt *ex vivo* kärlperfusionssystem utvecklats och utvärderats tekniskt såväl som biologiskt. Systemet kan bli ett viktigt redskap för att öka kunskapen kring mekaniska krafters reglerande effekter på endotelceller såväl som intakta humana kärl. Mekaniska krafter i kombination med eller utan inflammation har viktiga reglerande effekter på centrala hemostasgener, däribland det fibrinolytiska enzymet t-PA. En ogynnsam flödesprofil ökar vulnerabiliteten för inflammatorisk stress lokalt vilket medför ökad risk för atherotrombotiska händelser.

ACKNOWLEDGEMENT

I wish to express my sincere gratitude and appreciation to all who have contributed to this thesis in one way or another. In particular, I would like to thank:

Lena Karlsson, my supervisor, for your generous support and devotion, encouragement and great enthusiasm. Thank you for your never-ending inspiration and friendship. Your faith in me and my project helped me see the light at the end of the tunnel.

Sverker Jern, head of the Clinical Experimental Research Laboratory and my co-supervisor, for welcoming me to the research group and for all your support and encouragement during these years. Your vast knowledge in the field of vascular research and research methodology has been a great source of inspiration!

Erik Ulfhammer, for discussions about cell culture, analyzing techniques and your immense endurance and meticulousness when it comes to manuscript writing!

Mikael Ekman, for fruitful discussions and great team-work. We managed to find solutions to most of the problems we encountered!

Karl Swedberg, chairman of the Department of Emergency and Cardiovascular Medicine, Sahlgrenska University Hospital/Östra Gothenburg, for support and for providing resources.

Eva Thydén for excellent secretary skills, your kindness and endless support until the last minute!

Hannele Korhonen for brilliant laboratory assistance, *Cecilia Lundholm, Karolina Sandell, Sandra Huskanovic, Ulrika Nimblad, Ola Söderqvist and Katarina Glise* for excellent collaboration and for showing interest in the perfusion system.

My present and former colleagues, including co-authors and friends at the Clinical Experimental Research Laboratory, you made my Ph.D. studies a very pleasant time: *Helén Brogren, Pia Larsson, Maria Carlström, Ott Saluveer, Karin Wallmark, Mia Magnusson, Wilhelm Ridderstråle, Thórdís Hrafnkelsdóttir, Anna Wolf, Per Ladenvall, Claes Ladenvall, Christina Jern, Katarina Jood, Linda Olsson, Smita DuttaRoy, Thorarinn Gudnason* and all other people working in the group for longer and shorter periods.

Present nurses at the Clinical Experimental Research Laboratory for creating a pleasant atmosphere, especially *Lillian Alnäs, Annika Odenstedt, Sven-Eric Hägelind, Jonna Norman, Kim Fahlén, Helena Svensson* and *Görel Hultsberg Olsson.*

My family, and especially my mother, *Anne-Louise*, for always supporting, encouraging and believing in me. My father, *Claes-Håkan*, for introducing me to the field of medicine and giving me the willpower and energy to write this thesis, for our dialogues during evening walks and for your endless love. My brothers, *Henrik* and *Johan*, and my grandmother, *Britta*, for lending a helping hand in different stages of life.

My stepdaughter, *Daniella* for putting up with me working at home.

My children, *Filippa* and *Albin*, for all the joy and happiness you bring me.

My beloved wife, *Camilla*, for your support and endless love.

These studies were supported by grants from the Swedish Research Council, the Swedish Heart Lung Foundation, the Swedish Hypertension Society, the Sahlgrenska University Hospital Foundation and Emelle Foundation.

REFERENCES

1. Murray CJ, Lopez AD. Alternative projections of mortality and disability by cause 1990-2020: Global Burden of Disease Study. *Lancet* 1997; 349(9064):1498-1504.

2. Reinhart WH. Shear-dependence of endothelial functions. *Experientia* 1994; 50(2):87-93.

3. Jaffe EA. Cell biology of endothelial cells. *Hum Pathol* 1987; 18(3):234-239.

4. Pries AR, Secomb TW, Gaehtgens P. The endothelial surface layer. *Pflugers Arch* 2000; 440(5):653-666.

5. Lupu C, Kruithof EK, Kakkar VV, Lupu F. Acute release of tissue factor pathway inhibitor after in vivo thrombin generation in baboons. *Thromb Haemost* 1999; 82(6):1652-1658.

6. Emeis JJ. Regulation of the acute release of tissue-type plasminogen activator from the endothelium by coagulation activation products. *Ann N Y Acad Sci* 1992; 667:249-258.

7. van den Eijnden-Schrauwen Y, Kooistra T, de Vries RE, Emeis JJ. Studies on the acute release of tissue-type plasminogen activator from human endothelial cells in vitro and in rats in vivo: evidence for a dynamic storage pool. *Blood* 1995; 85(12):3510-3517.

8. Camoin L, Pannell R, Anfosso F, Lefevre JP, Sampol J, Gurewich V, Dignat-George F. Evidence for the expression of urokinase-type plasminogen activator by human venous endothelial cells in vivo. *Thromb Haemost* 1998; 80(6):961-967.

9. Madge LA, Pober JS. TNF signaling in vascular endothelial cells. *Exp Mol Pathol* 2001; 70(3):317-325.

10. Chobanian AV. Vascular effects of systemic hypertension. *Am J Cardiol* 1992; 69(13):3E-7E.

11. Dzau VJ, Gibbons GH. Vascular remodeling: mechanisms and implications. *J Cardiovasc Pharmacol* 1993; 21 Suppl 1:S1-5.

12. Gibbons GH, Dzau VJ. The emerging concept of vascular remodeling. *N Engl J Med* 1994; 330(20):1431-1438.

13. Glagov S. Intimal hyperplasia, vascular modeling, and the restenosis problem. *Circulation* 1994; 89(6):2888-2891.

14. Sjogren LS, Doroudi R, Gan L, Jungersten L, Hrafnkelsdottir T, Jern S. Elevated intraluminal pressure inhibits vascular tissue plasminogen activator secretion and downregulates its gene expression. *Hypertension* 2000; 35(4):1002-1008.

15. Sjogren LS, Gan L, Doroudi R, Jern C, Jungersten L, Jern S. Fluid shear stress increases the intra-cellular storage pool of tissue-type plasminogen activator in intact human conduit vessels. *Thromb Haemost* 2000; 84(2):291-298.

16. Davies PF. Flow-mediated endothelial mechanotransduction. *Physiol Rev* 1995; 75(3):519-560.

17. Malek AM, Izumo S. Molecular aspects of signal transduction of shear stress in the endothelial cell. *J Hypertens* 1994; 12(9):989-999.

18. Dobrin PB. Mechanical properties of arterises. *Physiol Rev* 1978; 58(2):397-460.

19. Ali MH, Schumacker PT. Endothelial responses to mechanical stress: where is the mechanosensor? *Crit Care Med* 2002; 30(5 Suppl):S198-206.

20. Resnick N, Yahav H, Shay-Salit A, Shushy M, Schubert S, Zilberman LC, Wofovitz E. Fluid shear stress and the vascular endothelium: for better and for worse. *Prog Biophys Mol Biol* 2003; 81(3):177-199.

21. Lehoux S, Castier Y, Tedgui A. Molecular mechanisms of the vascular responses to haemodynamic forces. *J Intern Med* 2006; 259(4):381-392.

22. Bergbrant A, Hansson L, Jern S. Interrelation of cardiac and vascular structure in young men with borderline hypertension. *Eur Heart J* 1993; 14(10):1304-1314.

23. Jern S, Wall U, Bergbrant A, Selin-Sjogren L, Jern C. Endothelium-dependent vasodilation and tissue-type plasminogen activator release in borderline hypertension. *Arterioscler Thromb Vasc Biol* 1997; 17(12):3376-3383.

24. Diamond SL, Eskin SG, McIntire LV. Fluid flow stimulates tissue plasminogen activator secretion by cultured human endothelial cells. *Science (New York, NY* 1989; 243(4897):1483-1485.

25. Inoue H, Taba Y, Miwa Y, Yokota C, Miyagi M, Sasaguri T. Transcriptional and posttranscriptional regulation of cyclooxygenase-2 expression by fluid shear stress in vascular endothelial cells. *Arterioscler Thromb Vasc Biol* 2002; 22(9):1415-1420.

26. Duerrschmidt N, Stielow C, Muller G, Pagano PJ, Morawietz H. NO-mediated regulation of NAD(P)H oxidase by laminar shear stress in human endothelial cells. *J Physiol* 2006; 576(Pt 2):557-567.

27. Hermann C, Zeiher AM, Dimmeler S. Shear stress inhibits H_2O_2-induced apoptosis of human endothelial cells by modulation of the glutathione redox cycle and nitric oxide synthase. *Arterioscler Thromb Vasc Biol* 1997; 17(12):3588-3592.

28. Ulfhammer E, Ridderstrale W, Andersson M, Karlsson L, Hrafnkelsdottir T, Jern S. Prolonged cyclic strain impairs the fibrinolytic system in cultured vascular endothelial cells. *J Hypertens* 2005; 23(8):1551-1557.

29. Sorop O, Spaan JA, VanBavel E. Pulsation-induced dilation of subendocardial and subepicardial arterioles: effect on vasodilator sensitivity. *Am J Physiol Heart Circ Physiol* 2002; 282(1):H311-319.

30. Ziegler T, Bouzourene K, Harrison VJ, Brunner HR, Hayoz D. Influence of oscillatory and unidirectional flow environments on the expression of endothelin and nitric oxide synthase in cultured endothelial cells. *Arterioscler Thromb Vasc Biol* 1998; 18(5):686-692.

31. Blackman BR, Garcia-Cardena G, Gimbrone MA, Jr. A new in vitro model to evaluate differential responses of endothelial cells to simulated arterial shear stress waveforms. *J Biomech Eng* 2002; 124(4):397-407.

32. Dai G, Kaazempur-Mofrad MR, Natarajan S, Zhang Y, Vaughn S, Blackman BR, Kamm RD, Garcia-Cardena G, Gimbrone MA, Jr. Distinct endothelial phenotypes evoked by arterial waveforms derived from atherosclerosis-susceptible and -resistant regions of human vasculature. *Proc Natl Acad Sci U S A* 2004; 101(41):14871-14876.

33. Bao X, Lu C, Frangos JA. Temporal gradient in shear but not steady shear stress induces PDGF-A and MCP-1 expression in endothelial cells: role of NO, NF kappa B, and egr-1. *Arterioscler Thromb Vasc Biol* 1999; 19(4):996-1003.

34. Peng X, Haldar S, Deshpande S, Irani K, Kass DA. Wall stiffness suppresses Akt/eNOS and cytoprotection in pulse-perfused endothelium. *Hypertension* 2003; 41(2):378-381.

35. Qiu Y, Tarbell JM. Interaction between wall shear stress and circumferential strain affects endothelial cell biochemical production. *J Vasc Res* 2000; 37(3):147-157.

36. Hutcheson IR, Griffith TM. Release of endothelium-derived relaxing factor is modulated both by frequency and amplitude of pulsatile flow. *Am J Physiol* 1991; 261(1 Pt 2):H257-262.

37. Mitchell GF. Pulse pressure, arterial compliance and cardiovascular morbidity and mortality. *Curr Opin Nephrol Hypertens* 1999; 8(3):335-342.

38. Ceravolo R, Maio R, Pujia A, Sciacqua A, Ventura G, Costa MC, Sesti G, Perticone F. Pulse pressure and endothelial dysfunction in never-treated hypertensive patients. *J Am Coll Cardiol* 2003; 41(10):1753-1758.

39. Malek AM, Alper SL, Izumo S. Hemodynamic shear stress and its role in atherosclerosis. *Jama* 1999; 282(21):2035-2042.

40. Bonetti PO, Holmes DR, Jr., Lerman A, Barsness GW. Enhanced external counterpulsation for ischemic heart disease: what's behind the curtain? *J Am Coll Cardiol* 2003; 41(11):1918-1925.

41. Hambrecht R, Wolf A, Gielen S, Linke A, Hofer J, Erbs S, Schoene N, Schuler G. Effect of exercise on coronary endothelial function in patients with coronary artery disease. *N Engl J Med* 2000; 342(7):454-460.

42. Hambrecht R, Adams V, Erbs S, Linke A, Krankel N, Shu Y, Baither Y, Gielen S, Thiele H, Gummert JF, Mohr FW, Schuler G. Regular physical activity improves endothelial function in patients with coronary artery disease by increasing phosphorylation of endothelial nitric oxide synthase. *Circulation* 2003; 107(25):3152-3158.

43. Gokce N, Vita JA, Bader DS, Sherman DL, Hunter LM, Holbrook M, O'Malley C, Keaney JF, Jr., Balady GJ. Effect of exercise on upper and lower extremity endothelial function in patients with coronary artery disease. *Am J Cardiol* 2002; 90(2):124-127.

44. Esmon CT. The interactions between inflammation and coagulation. *Br J Haematol* 2005; 131(4):417-430.

45. del Rincon ID, Williams K, Stern MP, Freeman GL, Escalante A. High incidence of cardiovascular events in a rheumatoid arthritis cohort not explained by traditional cardiac risk factors. *Arthritis Rheum* 2001; 44(12):2737-2745.

46. Goodson NJ, Wiles NJ, Lunt M, Barrett EM, Silman AJ, Symmons DP. Mortality in early inflammatory polyarthritis: cardiovascular mortality is increased in seropositive patients. *Arthritis Rheum* 2002; 46(8):2010-2019.

47. Willerson JT, Ridker PM. Inflammation as a cardiovascular risk factor. *Circulation* 2004; 109(21 Suppl 1):II2-10.

48. Jacobsson LT, Turesson C, Gulfe A, Kapetanovic MC, Petersson IF, Saxne T, Geborek P. Treatment with tumor necrosis factor blockers is associated with a lower incidence of first cardiovascular events in patients with rheumatoid arthritis. *J Rheumatol* 2005; 32(7):1213-1218.

49. Pober JS. Endothelial activation: intracellular signaling pathways. *Arthritis Res* 2002; 4 Suppl 3:S109-116.

50. Baud V, Karin M. Signal transduction by tumor necrosis factor and its relatives. *Trends Cell Biol* 2001; 11(9):372-377.

51. Kyriakis JM. Activation of the AP-1 transcription factor by inflammatory cytokines of the TNF family. *Gene Expr* 1999; 7(4-6):217-231.

52. Chiu JJ, Lee PL, Chang SF, Chen LJ, Lee CI, Lin KM, Usami S, Chien S. Shear stress regulates gene expression in vascular endothelial cells in response to tumor necrosis factor-alpha: a study of the transcription profile with complementary DNA microarray. *J Biomed Sci* 2005; 12(3):481-502.

53. Chiu JJ, Lee PL, Chen CN, Lee CI, Chang SF, Chen LJ, Lien SC, Ko YC, Usami S, Chien S. Shear stress increases ICAM-1 and decreases VCAM-1 and E-selectin expressions induced by tumor necrosis factor-[alpha] in endothelial cells. *Arterioscler Thromb Vasc Biol* 2004; 24(1):73-79.

54. Partridge J, Carlsen H, Enesa K, Chaudhury H, Zakkar M, Luong L, Kinderlerer A, Johns M, Blomhoff R, Mason JC, Haskard DO, Evans PC. Laminar shear stress acts as a switch to regulate divergent functions of NF-kappaB in endothelial cells. *FASEB J* 2007; 21(13):3553-3561.

55. Tsou JK, Gower RM, Ting HJ, Schaff UY, Insana MF, Passerini AG, Simon SI. Spatial regulation of inflammation by human aortic endothelial cells in a linear gradient of shear stress. *Microcirculation* 2008; 15(4):311-323.

56. Yamawaki H, Lehoux S, Berk BC. Chronic physiological shear stress inhibits tumor necrosis factor-induced proinflammatory responses in rabbit aorta perfused ex vivo. *Circulation* 2003; 108(13):1619-1625.

57. Bergh N, Ulfhammer E, Karlsson L, Jern S. Effects of two complex hemodynamic stimulation profiles on hemostatic genes in a vessel-like environment. *Endothelium* 2008; 15(5-6):231-238.

58. Ulfhammer E, Larsson P, Karlsson L, Hrafnkelsdottir T, Bokarewa M, Tarkowski A, Jern S. TNF-alpha mediated suppression of tissue type plasminogen activator expression in vascular endothelial cells is NF-kappaB- and p38 MAPK-dependent. *J Thromb Haemost* 2006; 4(8):1781-1789.

59. Kawai Y, Matsumoto Y, Watanabe K, Yamamoto H, Satoh K, Murata M, Handa M, Ikeda Y. Hemodynamic forces modulate the effects of cytokines on fibrinolytic activity of endothelial cells. *Blood* 1996; 87(6):2314-2321.

60. Brommer EJ. The level of extrinsic plasminogen activator (t-PA) during clotting as a determinant of the rate of fibrinolysis; inefficiency of activators added afterwards. *Thromb Res* 1984; 34(2):109-115.

61. Collen D. On the regulation and control of fibrinolysis. Edward Kowalski Memorial Lecture. *Thromb Haemost* 1980; 43(2):77-89.

62. Fox KA, Robison AK, Knabb RM, Rosamond TL, Sobel BE, Bergmann SR. Prevention of coronary thrombosis with subthrombolytic doses of tissue-type plasminogen activator. *Circulation* 1985; 72(6):1346-1354.

63. Lijnen HR, Collen D. Endothelium in hemostasis and thrombosis. *Prog Cardiovasc Dis* 1997; 39(4):343-350.

64. Kruithof EK, Tran-Thang C, Ransijn A, Bachmann F. Demonstration of a fast-acting inhibitor of plasminogen activators in human plasma. *Blood* 1984; 64(4):907-913.

65. Verheijen JH, Chang GT, Kluft C. Evidence for the occurrence of a fast-acting inhibitor for tissue-type plasminogen activator in human plasma. *Thromb Haemost* 1984; 51(3):392-395.

66. Bennett B, Croll A, Ferguson K, Booth NA. Complexing of tissue plasminogen activator with PAI-1, alpha 2-macroglobulin, and C1-inhibitor: studies in patients with defibrination and a fibrinolytic state after electroshock or complicated labor. *Blood* 1990; 75(3):671-676.

67. Booth NA, Walker E, Maughan R, Bennett B. Plasminogen activator in normal subjects after exercise and venous occlusion: t-PA circulates as complexes with C1-inhibitor and PAI-1. *Blood* 1987; 69(6):1600-1604.

68. Matsuno H, Kozawa O, Niwa M, Ueshima S, Matsuo O, Collen D, Uematsu T. Differential role of components of the fibrinolytic system in the formation and removal of thrombus induced by endothelial injury. *Thromb Haemost* 1999; 81(4):601-604.

69. Kathiresan S, Yang Q, Larson MG, Camargo AL, Tofler GH, Hirschhorn JN, Gabriel SB, O'Donnell CJ. Common genetic variation in five thrombosis genes and relations to plasma hemostatic protein level and cardiovascular disease risk. *Arterioscler Thromb Vasc Biol* 2006; 26(6):1405-1412.

70. Kooistra T, Schrauwen Y, Arts J, Emeis JJ. Regulation of endothelial cell t-PA synthesis and release. *Int J Hematol* 1994; 59(4):233-255.

71. Eliasson M, Hagg E, Lundblad D, Karlsson R, Bucht E. Influence of smoking and snuff use on electrolytes, adrenal and calcium regulating hormones. *Acta Endocrinol (Copenh)* 1993; 128(1):35-40.

72. Eliasson M, Jansson JH, Nilsson P, Asplund K. Increased levels of tissue plasminogen activator antigen in essential hypertension. A population-based study in Sweden. *J Hypertens* 1997; 15(4):349-356.

73. Jern S, Selin L, Bergbrant A, Jern C. Release of tissue-type plasminogen activator in response to muscarinic receptor stimulation in human forearm. *Thromb Haemost* 1994; 72(4):588-594.

74. Chandler WL, Alessi MC, Aillaud MF, Henderson P, Vague P, Juhan-Vague I. Clearance of tissue plasminogen activator (TPA) and TPA/plasminogen activator inhibitor type 1 (PAI-1) complex: relationship to elevated TPA antigen in patients with high PAI-1 activity levels. *Circulation* 1997; 96(3):761-768.

75. Dobrovolsky AB, Titaeva EV. The fibrinolysis system: regulation of activity and physiologic functions of its main components. *Biochemistry (Mosc)* 2002; 67(1):99-108.

76. Alfano D, Franco P, Vocca I, Gambi N, Pisa V, Mancini A, Caputi M, Carriero MV, Iaccarino I, Stoppelli MP. The urokinase plasminogen activator and its receptor: role in cell growth and apoptosis. *Thromb Haemost* 2005; 93(2):205-211.

77. Choong PF, Nadesapillai AP. Urokinase plasminogen activator system: a multifunctional role in tumor progression and metastasis. *Clin Orthop Relat Res* 2003; (415 Suppl):S46-58.

78. Kienast J, Padro T, Steins M, Li CX, Schmid KW, Hammel D, Scheld HH, van de Loo JC. Relation of urokinase-type plasminogen activator expression to presence and severity of atherosclerotic lesions in human coronary arteries. *Thromb Haemost* 1998; 79(3):579-586.

79. Binder BR, Mihaly J, Prager GW. uPAR-uPA-PAI-1 interactions and signaling: a vascular biologist's view. *Thromb Haemost* 2007; 97(3):336-342.

80. Crippa MP. Urokinase-type plasminogen activator. *Int J Biochem Cell Biol* 2007; 39(4):690-694.

81. Lupu F, Heim DA, Bachmann F, Hurni M, Kakkar VV, Kruithof EK. Plasminogen activator expression in human atherosclerotic lesions. *Arterioscler Thromb Vasc Biol* 1995; 15(9):1444-1455.

82. Raghunath PN, Tomaszewski JE, Brady ST, Caron RJ, Okada SS, Barnathan ES. Plasminogen activator system in human coronary atherosclerosis. *Arterioscler Thromb Vasc Biol* 1995; 15(9):1432-1443.

83. Niedbala MJ, Stein M. Tumor necrosis factor induction of urokinase-type plasminogen activator in human endothelial cells. *Biomed Biochim Acta* 1991; 50(4-6):427-436.

84. Falkenberg M, Tom C, DeYoung MB, Wen S, Linnemann R, Dichek DA. Increased expression of urokinase during atherosclerotic lesion development causes arterial constriction and lumen loss, and accelerates lesion growth. *Proc Natl Acad Sci U S A* 2002; 99(16):10665-10670.

85. Lijnen HR. Extracellular proteolysis in the development and progression of atherosclerosis. *Biochem Soc Trans* 2002; 30(2):163-167.

86. Rijken DC. Plasminogen activators and plasminogen activator inhibitors: biochemical aspects. *Baillieres Clin Haematol* 1995; 8(2):291-312.

87. Booth NA, Simpson AJ, Croll A, Bennett B, MacGregor IR. Plasminogen activator inhibitor (PAI-1) in plasma and platelets. *Br J Haematol* 1988; 70(3):327-333.

88. Declerck PJ, Alessi MC, Verstreken M, Kruithof EK, Juhan-Vague I, Collen D. Measurement of plasminogen activator inhibitor 1 in biologic fluids with a murine monoclonal antibody-based enzyme-linked immunosorbent assay. *Blood* 1988; 71(1):220-225.

89. Juhan-Vague I, Pyke SD, Alessi MC, Jespersen J, Haverkate F, Thompson SG. Fibrinolytic factors and the risk of myocardial infarction or sudden death in patients with angina pectoris. ECAT Study Group. European Concerted Action on Thrombosis and Disabilities. *Circulation* 1996; 94(9):2057-2063.

90. Booth NA. Fibrinolysis and thrombosis. *Baillieres Best Pract Res Clin Haematol* 1999; 12(3):423-433.

91. Lucore CL, Fujii S, Wun TC, Sobel BE, Billadello JJ. Regulation of the expression of type 1 plasminogen activator inhibitor in Hep G2 cells by epidermal growth factor. *J Biol Chem* 1988; 263(31):15845-15848.

92. Sawdey MS, Loskutoff DJ. Regulation of murine type 1 plasminogen activator inhibitor gene expression in vivo. Tissue specificity and induction by lipopolysaccharide, tumor necrosis factor-alpha, and transforming growth factor-beta. *J Clin Invest* 1991; 88(4):1346-1353.

93. Simpson AJ, Booth NA, Moore NR, Bennett B. Distribution of plasminogen activator inhibitor (PAI-1) in tissues. *J Clin Pathol* 1991; 44(2):139-143.

94. Brogren H, Karlsson L, Andersson M, Wang L, Erlinge D, Jern S. Platelets synthesize large amounts of active plasminogen activator inhibitor 1. *Blood* 2004; 104(13):3943-3948.

95. Brogren H, Sihlbom C, Wallmark K, Lonn M, Deinum J, Karlsson L, Jern S. Heterogeneous glycosylation patterns of human PAI-1 may reveal its cellular origin. *Thromb Res* 2008; 122(2):271-281.

96. Schleef RR, Podor TJ, Dunne E, Mimuro J, Loskutoff DJ. The majority of type 1 plasminogen activator inhibitor associated with cultured human endothelial cells is located under the cells and is accessible to solution-phase tissue-type plasminogen activator. *J Cell Biol* 1990; 110(1):155-163.

97. Huber K. Plasminogen activator inhibitor type-1 (part one): basic mechanisms, regulation, and role for thromboembolic disease. *J Thromb Thrombolysis* 2001; 11(3):183-193.

98. Alessi MC, Juhan-Vague I. PAI-1 and the metabolic syndrome: links, causes, and consequences. *Arterioscler Thromb Vasc Biol* 2006; 26(10):2200-2207.

99. Juhan-Vague I, Alessi MC, Mavri A, Morange PE. Plasminogen activator inhibitor-1, inflammation, obesity, insulin resistance and vascular risk. *J Thromb Haemost* 2003; 1(7):1575-1579.

100. Dahlback B, Villoutreix BO. Regulation of blood coagulation by the protein C anticoagulant pathway: novel insights into structure-function relationships and molecular recognition. *Arterioscler Thromb Vasc Biol* 2005; 25(7):1311-1320.

101. Van de Wouwer M, Collen D, Conway EM. Thrombomodulin-protein C-EPCR system: integrated to regulate coagulation and inflammation. *Arterioscler Thromb Vasc Biol* 2004; 24(8):1374-1383.

102. Wu KK. Regulation of endothelial nitric oxide synthase activity and gene expression. *Ann N Y Acad Sci* 2002; 962:122-130.

103. Kuhlencordt PJ, Gyurko R, Han F, Scherrer-Crosbie M, Aretz TH, Hajjar R, Picard MH, Huang PL. Accelerated atherosclerosis, aortic aneurysm formation, and ischemic heart disease in apolipoprotein E/endothelial nitric oxide synthase double-knockout mice. *Circulation* 2001; 104(4):448-454.

104. Shesely EG, Maeda N, Kim HS, Desai KM, Krege JH, Laubach VE, Sherman PA, Sessa WC, Smithies O. Elevated blood pressures in mice lacking endothelial nitric oxide synthase. *Proc Natl Acad Sci U S A* 1996; 93(23):13176-13181.

105. Preiss DJ, Sattar N. Vascular cell adhesion molecule-1: a viable therapeutic target for atherosclerosis? *Int J Clin Pract* 2007; 61(4):697-701.

106. Cybulsky MI, Iiyama K, Li H, Zhu S, Chen M, Iiyama M, Davis V, Gutierrez-Ramos JC, Connelly PW, Milstone DS. A major role for VCAM-1, but not ICAM-1, in early atherosclerosis. *J Clin Invest* 2001; 107(10):1255-1262.

107. Blankenberg S, Barbaux S, Tiret L. Adhesion molecules and atherosclerosis. *Atherosclerosis* 2003; 170(2):191-203.

108. Gan L, Sjogren LS, Doroudi R, Jern S. A new computerized biomechanical perfusion model for ex vivo study of fluid mechanical forces in intact conduit vessels. *J Vasc Res* 1999; 36(1):68-78.

109. VanBavel E, Mooij T, Giezeman MJ, Spaan JA. Cannulation and continuous cross-sectional area measurement of small blood vessels. *Journal of pharmacological methods* 1990; 24(3):219-227.

110. Jaffe EA, Nachman RL, Becker CG, Minick CR. Culture of human endothelial cells derived from umbilical veins. Identification by morphologic and immunologic criteria. *J Clin Invest* 1973; 52(11):2745-2756.

111. Cooke BM, Usami S, Perry I, Nash GB. A simplified method for culture of endothelial cells and analysis of adhesion of blood cells under conditions of flow. *Microvasc Res* 1993; 45(1):33-45.

112. Peng X, Recchia FA, Byrne BJ, Wittstein IS, Ziegelstein RC, Kass DA. In vitro system to study realistic pulsatile flow and stretch signaling in cultured vascular cells. *Am J Physiol Cell Physiol* 2000; 279(3):C797-805.

113. Higuchi R, Fockler C, Dollinger G, Watson R. Kinetic PCR analysis: real-time monitoring of DNA amplification reactions. *Biotechnology (N Y)* 1993; 11(9):1026-1030.

114. Lux W, Klobeck HG, Daniel PB, Costa M, Medcalf RL, Schleuning WD. In vivo and in vitro analysis of the human tissue-type plasminogen activator gene promoter in neuroblastomal cell lines: evidence for a functional upstream kappaB element. *J Thromb Haemost* 2005; 3(5):1009-1017.

115. Costa M, Shen Y, Maurer F, Medcalf RL. Transcriptional regulation of the tissue-type plasminogen-activator gene in human endothelial cells: identification of nuclear factors that recognise functional elements in the tissue-type plasminogen-activator gene promoter. *Eur J Biochem* 1998; 258(1):123-131.

116. Resnick N, Collins T, Atkinson W, Bonthron DT, Dewey CF, Jr., Gimbrone MA, Jr. Platelet-derived growth factor B chain promoter contains a cis-acting fluid shear-stress-responsive element. *Proc Natl Acad Sci U S A* 1993; 90(10):4591-4595.

117. Arts J, Herr I, Lansink M, Angel P, Kooistra T. Cell-type specific DNA-protein interactions at the tissue-type plasminogen activator promoter in human endothelial and HeLa cells in vivo and in vitro. *Nucleic Acids Res* 1997; 25(2):311-317.

118. Osborn L, Kunkel S, Nabel GJ. Tumor necrosis factor alpha and interleukin 1 stimulate the human immunodeficiency virus enhancer by activation of the nuclear factor kappa B. *Proc Natl Acad Sci U S A* 1989; 86(7):2336-2340.

119. Sambrock J. FE, Maniatis T. Molecular cloning: a laboratory manual. Cold Spring Harbor, New York. *Cold Spring Harbor Laboratory* 1989; 2nd edition.

120. Costa M, Medcalf RL. Differential binding of cAMP-responsive-element (CRE)-binding protein-1 and activating transcription factor-2 to a CRE-like element in the human tissue-type plasminogen activator (t-PA) gene promoter correlates with opposite regulation of t-PA by phorbol ester in HT-1080 and HeLa cells. *Eur J Biochem* 1996; 237(3):532-538.

121. Bardy N, Karillon GJ, Merval R, Samuel JL, Tedgui A. Differential effects of pressure and flow on DNA and protein synthesis and on fibronectin expression by arteries in a novel organ culture system. *Circ Res* 1995; 77(4):684-694.

122. Bolz SS, Pieperhoff S, De Wit C, Pohl U. Intact endothelial and smooth muscle function in small resistance arteries after 48 h in vessel culture. *Am J Physiol Heart Circ Physiol* 2000; 279(3):H1434-1439.

123. Bakker EN, van Der Meulen ET, Spaan JA, VanBavel E. Organoid culture of cannulated rat resistance arteries: effect of serum factors on vasoactivity and remodeling. *Am J Physiol Heart Circ Physiol* 2000; 278(4):H1233-1240.

124. Hendrickson RJ, Cappadona C, Yankah EN, Sitzmann JV, Cahill PA, Redmond EM. Sustained pulsatile flow regulates endothelial nitric oxide synthase and cyclooxygenase expression in co-cultured vascular endothelial and smooth muscle cells. *J Mol Cell Cardiol* 1999; 31(3):619-629.

125. Nackman GB, Fillinger MF, Shafritz R, Wei T, Graham AM. Flow modulates endothelial regulation of smooth muscle cell proliferation: a new model. *Surgery* 1998; 124(2):353-360; discussion 360-351.

126. Ziegler T, Alexander RW, Nerem RM. An endothelial cell-smooth muscle cell co-culture model for use in the investigation of flow effects on vascular biology. *Ann Biomed Eng* 1995; 23(3):216-225.

127. Oano Sorop JAES, and Ed Vanbavel. Pulsation-induced dilation of subendocardial and subepicardial arterioles: effect on vasodilator sensitivity. *Am J Physiol Heart Circ Physiol* 2002; 282:311-319.

128. McCormick SM, Eskin SG, McIntire LV, Teng CL, Lu CM, Russell CG, Chittur KK. DNA microarray reveals changes in gene expression of shear stressed human umbilical vein endothelial cells. *Proc Natl Acad Sci U S A* 2001; 98(16):8955-8960.

129. Chen BP, Li YS, Zhao Y, Chen KD, Li S, Lao J, Yuan S, Shyy JY, Chien S. DNA microarray analysis of gene expression in endothelial cells in response to 24-h shear stress. *Physiol Genomics* 2001; 7(1):55-63.

130. Frye SR, Yee A, Eskin SG, Guerra R, Cong X, Mcintire LV. cDNA microarray analysis of endothelial cells subjected to cyclic mechanical strain: importance of motion control. *Physiol Genomics* 2005; 21:124-130.

131. Riha GM, Lin PH, Lumsden AB, Yao Q, Chen C. Roles of hemodynamic forces in vascular cell differentiation. *Ann Biomed Eng* 2005; 33(6):772-779.

132. Lehoux S, Tedgui A. Cellular mechanics and gene expression in blood vessels. *J Biomech* 2003; 36(5):631-643.

133. Khayutin VM, Lukoshkova EV, Rogoza AN, Nikolsky VP. Negative feedbacks in the pathogenesis of primary arterial hypertension: mechanosensitivity of the endothelium. *Blood pressure* 1995; 4(2):70-76.

134. Diamond SL, Sharefkin JB, Dieffenbach C, Frasier-Scott K, McIntire LV, Eskin SG. Tissue plasminogen activator messenger RNA levels increase in cultured human endothelial cells exposed to laminar shear stress. *J Cell Physiol* 1990; 143(2):364-371.

135. Malek AM, Jackman R, Rosenberg RD, Izumo S. Endothelial expression of thrombomodulin is reversibly regulated by fluid shear stress. *Circ Res* 1994; 74(5):852-860.

136. Hrafnkelsdottir T, Wall U, Jern C, Jern S. Impaired capacity for endogenous fibrinolysis in essential hypertension. *Lancet* 1998; 352(9140):1597-1598.

137. Ridderstrale W, Ulfhammer E, Jern S, Hrafnkelsdottir T. Impaired capacity for stimulated fibrinolysis in primary hypertension is restored by antihypertensive therapy. *Hypertension* 2006; 47(4):686-691.

138. Metallo CM, Vodyanik MA, de Pablo JJ, Slukvin, II, Palecek SP. The response of human embryonic stem cell-derived endothelial cells to shear stress. *Biotechnology and bioengineering* 2008; 100(4):830-837.

139. Surapisitchat J, Hoefen RJ, Pi X, Yoshizumi M, Yan C, Berk BC. Fluid shear stress inhibits TNF-alpha activation of JNK but not ERK1/2 or p38 in human umbilical vein endothelial cells: Inhibitory crosstalk among MAPK family members. *Proc Natl Acad Sci U S A* 2001; 98(11):6476-6481.

140. Mohan S, Mohan N, Sprague EA. Differential activation of NF-kappa B in human aortic endothelial cells conditioned to specific flow environments. *Am J Physiol* 1997; 273(2 Pt 1):C572-578.

141. Traub O, Berk BC. Laminar shear stress: mechanisms by which endothelial cells transduce an atheroprotective force. *Arterioscler Thromb Vasc Biol* 1998; 18(5):677-685.

142. Frye SR, Yee A, Eskin SG, Guerra R, Cong X, McIntire LV. cDNA microarray analysis of endothelial cells subjected to cyclic mechanical strain: importance of motion control. *Physiological genomics* 2005; 21(1):124-130.

ISBN 978-91-628-7891-7
Printed by Geson Hylte Tryck, Gothenburg